A critical review of the thermophysical properties and applications of carbon-based hybrid nanofluids in solar thermal systems

Adeola Borode*, Thato Tshephe and Peter Olubambi

Centre for Nanoengineering and Advanced Materials, School of Mining, Metallurgical and Chemical Engineering, University of Johannesburg, Johannesburg, South Africa

This review focuses on the potential of carbon-based hybrid nanofluids to enhance the performance of solar thermal energy systems. Solar thermal technology is pivotal in transitioning towards renewable energy sources, offering sustainable alternatives to conventional fossil fuels. However, traditional heat transfer fluids (HTFs) often exhibit limitations in thermal conductivity (TC), which hinders the overall efficiency of solar collectors. The introduction of nanofluids, particularly hybrid nanofluids that combine two or more types of nanoparticles, has emerged as a promising solution to address these challenges. Among various nanomaterials, carbon-based materials such as graphene and multi-walled carbon nanotubes (CNTs) have garnered significant attention due to their exceptional thermal properties. This review critically analyses the thermal and rheological characteristics of carbon-based hybrid nanofluids and their effects on solar thermal applications, including flat-plate collectors and parabolic trough collectors. The unique synergy achieved by integrating carbon-based nanoparticles with metallic nanoparticles results in improved TC, enhanced heat transfer rates, and greater stability compared to single-component nanofluids. Despite the notable advantages, challenges such as increased viscosity and the need for long-term stability under operational conditions remain pertinent. Future research directions should prioritize optimizing nanoparticle concentrations, exploring cost-effective alternatives, and investigating the long-term performance of hybrid nanofluids in dynamic environments. The findings of this review underscore the transformative potential of carbon-based hybrid nanofluids in improving the efficiency and effectiveness of solar thermal systems, thus supporting the broader adoption of renewable energy technologies. This exploration is essential for advancing solar thermal applications and addressing the ongoing challenges of energy sustainability and efficiency in the face of growing global energy demands.

KEYWORDS

carbon nanomaterial, hybrid nanofluid, carbon nanotube, graphene, solar collector, efficiency

1 Introduction

Solar thermal energy systems harness the sun's radiant energy to generate heat, playing a pivotal role in the transition toward renewable energy sources (Kassem et al., 2016). These systems offer a sustainable and environmentally friendly alternative to conventional fossil fuel-based energy generation, mitigating greenhouse gas emissions and promoting long-term energy security (Bellos et al., 2016; Patel et al., 2018). Solar thermal technology systems are particularly effective in regions with high solar irradiance, where they can significantly reduce dependence on conventional energy sources. The simplicity of solar thermal systems, combined with their ability to store thermal energy for later use, makes them an attractive option for residential and industrial applications.

Solar thermal energy systems can be utilized for specific applications, including water heating, space heating, industrial processes, and power generation (Bellos and Tzivanidis, 2017; Wang et al., 2016). These systems convert sunlight into thermal energy using solar collectors, which are designed to absorb and transfer heat to a working fluid. Common types of solar thermal systems include flat-plate collectors, evacuated tube collectors, and parabolic trough collectors, each optimized for different temperature ranges and applications. Figure 1 presents a classification of the different types of solar collectors.

Among various solar thermal collector technologies, parabolic trough collectors (PTCs) are notable for achieving high temperatures suitable for applications requiring substantial thermal energy (Hussein et al., 2024; Panchal et al., 2022). PTCs concentrate sunlight onto a receiver tube filled with a heat transfer fluid (HTF) using a parabolic reflector (Ajbar et al., 2023; Elshamy et al., 2021). Flat plate solar collectors (FPSCs) and evacuated tube solar collectors (ETSCs) also utilize HTF. FPSCs circulate it beneath a flat absorber plate made of copper or aluminum, effectively providing domestic hot water and space heating, although they operate at lower temperatures. In contrast, ETSCs enhance efficiency in colder climates by using a vacuum to minimize heat loss, containing a heat pipe or fluid-filled tube that absorbs solar radiation and transfers heat. The choice among these collector types depends on specific application needs, including temperature range and geographic location.

The heat transfer fluid (HTF), typically oil or water, absorbs concentrated solar radiation and transports thermal energy for use (AbdEl-Rady Abu-Zeid et al., 2024; Al-Rabeeah et al., 2022; Habchi et al., 2023). The efficiency of solar collectors is closely linked to the HTF's thermal conductivity (TC), which affects its ability to absorb and transfer heat (Asaad Yasseen et al., 2022). While conventional HTFs are affordable and accessible, they have limitations, such as relatively low TC, which restricts efficient heat absorption and transport. This results in elevated thermal losses and reduced system efficiency (AbdEl-Rady Abu-Zeid et al., 2024; Rovira et al., 2016). Additionally, conventional HTFs can degrade and become unstable at high temperatures, requiring frequent maintenance and reducing lifespan, which impacts economic viability. Their high viscosity can also increase pumping power requirements, further affecting energy efficiency and operational costs. To enhance thermal performance in PTCs, researchers are exploring nanotechnology, including nanofluids.

Nanofluids, which are suspensions of nanoparticles in a base fluid, have gained attention for their ability to enhance the performance of conventional heat transfer fluids. This is due to their superior thermal conductivity, stability, and heat transfer properties compared to traditional fluids, enabling more efficient energy management in various industrial and engineering applications (A.O. Borode et al., 2021). Incorporating high TC nanoparticles, such as metals or carbon nanotubes (CNTs), significantly improves heat absorption and transport, leading to faster heat transfer rates and better system efficiency (Ganvir et al., 2017). HNFs, which combine multiple types of nanoparticles, have shown particular effectiveness in enhancing thermal performance by leveraging the complementary properties of different materials (Ranga Babu et al., 2017). Carbon-based HNFs, combining carbon materials like graphene or carbon nanotubes with metallic nanoparticles, are especially promising due to their exceptional thermal properties (A.O. Borode et al., 2021). Carbon-based nanofluids demonstrate superior TC due to the intrinsic properties of carbon structures (A.O. Borode et al., 2021). When integrated into HNFs, these materials enhance heat transfer rates and stability, reducing the risk of particle agglomeration and sedimentation over time (Vărdaru et al., 2022). Moreover, nanofluids, especially carbon-based HNFs, allow for tunable viscosity (Babar et al., 2019), optimizing flow and heat transfer within the collector. Additionally, carbon-based nanoparticles can lower the specific heat of the working fluid, requiring less energy to achieve desired temperatures, thus further improving efficiency. Figure 2 illustrates various forms of carbon nanomaterials.

Extensive research has shown that nanofluids can outperform conventional fluids in thermal properties, and the synergistic effects of HNFs lead to even greater enhancements (Akhgar and Toghraie, 2018; Borode et al., 2023a; Zadkhast et al., 2017). This review comprehensively analyses carbon-based HNFs and their applications in solar thermal systems, highlighting the untapped potential in this area. It critically examines how combining carbon-based materials with metallic nanoparticles enhances the overall performance of solar thermal systems.

2 Thermophysical properties

The thermophysical properties of carbon-based HNFs have garnered significant attention in recent years, driven by their promising potential to enhance heat transfer processes across a variety of industrial applications. Key properties such as TC, viscosity, specific heat capacity (SHC), and density significantly impact the performance of nanofluids, and several studies have explored how hybridizing carbon-based nanoparticles with metallic or metal oxide particles can further optimize these properties.

2.1 Thermal conductivity

Thermal conductivity is a critical property that dictates the heat transfer capability of nanofluids. A defining characteristic of carbon-based HNFs is their remarkably high TC, surpassing that of both the base fluid and individual nanofluids (Akhgar and Toghraie, 2018; Soltani et al., 2020). This superior TC stems from the inherent

FIGURE 1
Classifications of solar collectors (Alam et al., 2021).
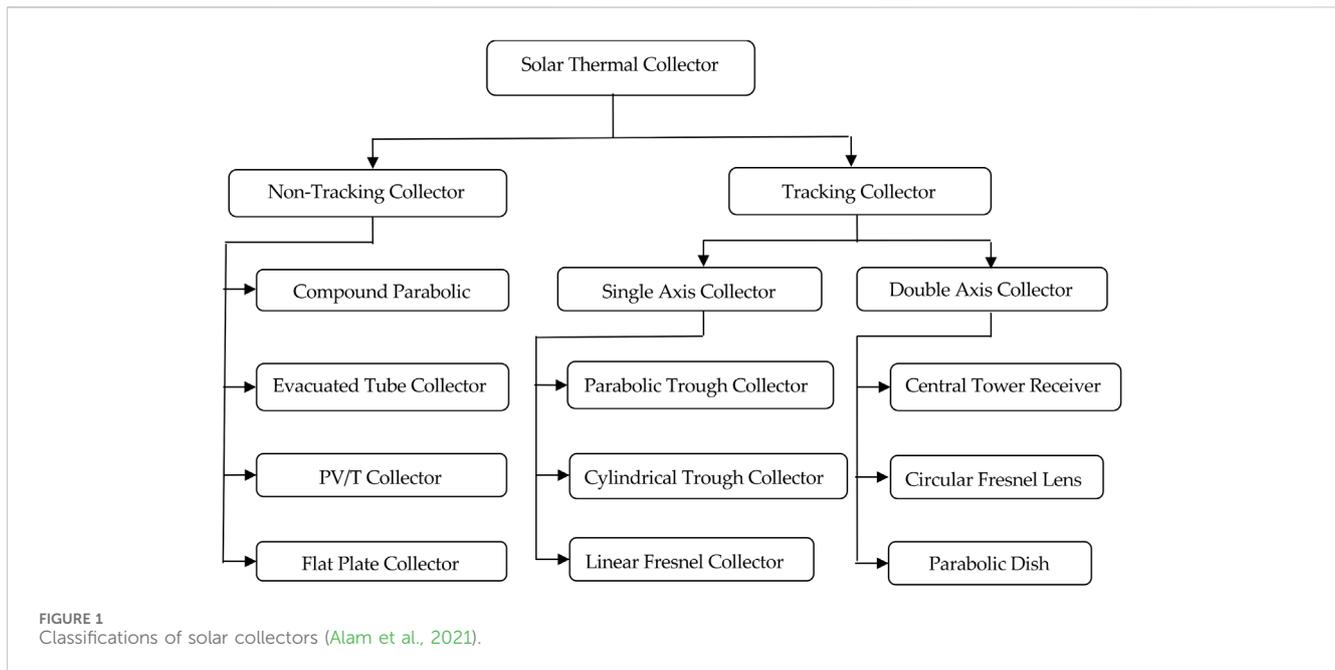
properties of carbon nanomaterials, particularly graphene or multi-walled carbon nanotube (MWCNT), renowned for its exceptional heat conduction capabilities (Kumar et al., 2021; Vărdaru et al., 2022). The incorporation of these nanomaterials into the base fluid creates a network of interconnected pathways that facilitate efficient heat transfer, enabling rapid absorption and transport of thermal energy from the concentrated solar radiation.

Several studies have showcased the remarkable TC enhancement achieved with carbon-based HNFs. For instance, (Borode et al., 2023b) reported up to 17.82% increase in TC in GNP-alumina HNFs across various concentrations. This improvement is largely attributed to the synergistic effect between the graphene's high TC and the alumina's ability to disperse heat within the base fluid effectively. However, a potential drawback in this study is the lack of focus on the long-term stability of the nanofluid. While initial increases in TC are promising, future studies should explore how stable these nanofluids remain over time, especially when used in dynamic systems where agglomeration may occur.

Jin et al. (2024) prepared HNFs using ethylene glycol (EG)/water (50:50) enhanced with graphene oxide (GO) and MXene (1:1) nanoparticles. Testing at temperatures between 20°C and 60°C revealed that both TC and viscosity increased with GO/MXene dosage. The nanofluid with 0.3 wt% GO/MXene demonstrated the largest TC enhancement of 33.49% at 60°C while maintaining low viscosity. In a separate study, Mehrali et al. (2017) characterized the thermophysical and magnetic properties of GNP/Fe_3O_4 HNFs, reporting an 11% enhancement in TC. Huminic et al. (2024) investigated the TC of silver nanoparticles-reduced graphene oxide dispersed in a water and ethylene glycol mixture (Ag NPs-rGO/W + EG). Their findings indicated that TC was influenced by both concentration and temperature, achieving a maximum enhancement of 1.13 times at 323.15 K and 0.10 wt% concentration compared to the base fluid.

Shahsavar et al. (2015) investigated a water-based hybrid nanofluid (HNF) containing Fe_3O_4 magnetic nanoparticles and CNTs. They found

that optimal TC enhancement, ranging from 13% to 34.26%, was achieved with 5 min of ultrasonication at temperatures between 25°C and 55°C compared to the base fluid. They observed that shorter sonication durations (e.g., 2.5 min) resulted in inadequate nanoparticle dispersion. In contrast, prolonged sonication compromised the CNTs' aspect ratio and network structure, thereby reducing the effectiveness of TC enhancement.

Vărdaru et al. (2023) studied the TC of water-based silver-reduced graphene oxide (Ag-rGO) nanofluids at varying concentrations and temperatures. They found that Ag-rGO nanofluids significantly enhanced TC compared to conventional liquids due to the high conductivity of solid nanoparticles. Adding 0.4 g/L of CMCNa surfactant to deionized water resulted in a minimal TC improvement of 0.703%. The TC increased with temperature, driven by enhanced Brownian motion, reduced viscosity, and increased particle collisions. At 20°C, TC enhancements for 0.050, 0.075, and 0.10 wt% Ag-rGO were 1.65%, 5.24%, and 8.39%, respectively, rising to 6.14%, 7.80%, and 10.69% at 50°C. This improvement is attributed to the formation of long Ag-rGO particle chains at higher temperatures, which create effective heat conduction pathways, and the deposition of silver nanoparticles on graphene oxide sheets, enhancing heat transfer within the nanofluid.

Alsangur et al. (2024) investigated the magnetic field-dependent TC of Fe_3O_4/CNT-water and Fe_3O_4/Graphene-water HNFs. They found that TC increased with magnetic field strength and particle concentration, with Fe_3O_4/Graphene-water showing up to three times greater enhancement than Fe_3O_4/CNT-water, achieving maximum TC improvements of approximately 12% and 9% for Fe_3O_4/CNT-water and 51% and 21% for Fe_3O_4/Graphene-water under parallel and perpendicular magnetic fields, respectively. Additionally, Srinivasan and Ponnusamy (2024) developed distilled water-based hybrid phase change materials (NFPCMs) using oxygen-functionalized graphene nanoplates and copper oxide nanoparticles, achieving maximum TC enhancements of
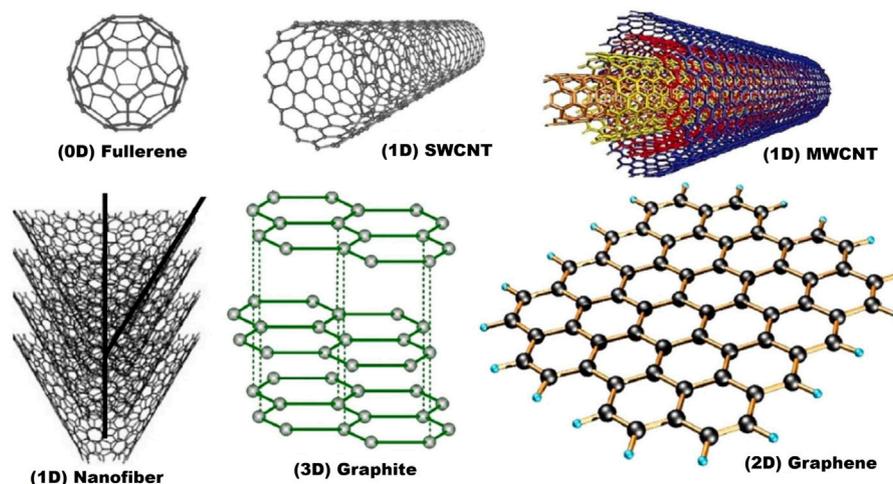
FIGURE 2
Various forms of Carbon nanomaterials (Atta et al., 2015).

30.75% in the solid state and 17.69% in the liquid state compared to the base PCM.

Vărdaru et al. (2022) investigated the TC of graphene oxide-silicon (GO-Si) HNFs in water at varying temperature ranges and mixture ratios, particularly at a concentration of 0.25 wt%. Their study revealed that TC increased with both temperature and GO concentration, consistently outperforming the base fluid. This is because higher temperatures enhanced molecular interactions, leading to more frequent collisions between molecules, which promoted energy transfer and improved heat conduction. HNFs with a higher GO content (0.8 GO: 0.2 Si) demonstrated better thermal performance than those with a higher Si content (0.2 GO: 0.8 Si), with maximum TC enhancement reaching 7.97% at elevated temperatures. The stability of the nanofluid and the high TC of the dispersed nanomaterials were crucial for these improvements. Additionally, the increased temperature enhanced the Brownian motion of nanoparticles, intensifying micro-convection and improving local mixing within the fluid.

Similarly, (Yarmand et al., 2016a) demonstrated that GNP-platinum (GNP-Pt) HNFs exhibited a 22.22% increase in TC at a 0.1 wt% nanoparticle concentration, attributed to platinum's high TC and graphene's large surface area. However, further concentration increases can lead to diminishing returns due to particle agglomeration and sedimentation, underscoring the need to optimize nanoparticle concentration in practical applications. Future research should aim to balance TC enhancement with the challenges of increased viscosity and sedimentation. Mehrali et al. (2018) demonstrated a 24% improvement in TC with graphene-silver HNFs. The enhanced performance is attributed to metallic particles, like silver, which create efficient thermal pathways. However, the high cost of silver limits its industrial scalability, raising concerns about its cost-effectiveness. Exploring more affordable alternatives, such as graphene-copper hybrids, could offer comparable thermal enhancements without the financial constraints of silver.

This body of research underscores the remarkable TC enhancements achieved with HNFs, which frequently outperform single-component nanofluids (mono NFs). The superior performance of HNFs arises from the synergistic interplay of multiple nanoparticles, leveraging their distinct properties to achieve enhanced heat transfer compared to mono NFs, which depend on the attributes of a single nanoparticle type. Comparative studies offer valuable insights to elucidate these differences. For instance, Soltani et al. (2020) investigated the TC of mono and HNFs, revealing different behaviors with temperature and volume fraction. Mono nanofluids like Oil/WO_3 and Oil/MWCNTs showed steady TC increases, with Oil/WO_3 rising by 11.45% and Oil/MWCNTs by 14.5% from 20°C to 60°C. HNFs like Oil/WO_3-MWCNTs, however, demonstrated superior performance. At 0.2% volume fraction, the hybrid reached 0.147 W/m·K at 60°C, a 5% increase, and at 0.6%, the TC improved by 19.55%. This highlights the synergistic effects of combined nanoparticles, as HNFs consistently outperformed mono nanofluids, demonstrating enhanced thermal performance.

Shajan et al. (2021) examined the TC of TH55-GNP/Al_2O_3 HNFs and compared them with GNP and Al_2O_3 mono-nanofluids. TC increased with nanoparticle concentration and temperature, with TH55-Al_2O_3 showing a maximum TC boost of 8.44% at 65°C and TH55-GNP achieving 15.69% at 0.1% concentration. HNFs performed better at higher GNP levels, with a maximum enhancement of 18.72% for TH55-GNP(0.1%)/Al_2O_3(1.0%). The improvement is due to enhanced micro-convection from Brownian motion and GNP platelets attaching to Al_2O_3 nanoparticles, improving heat transfer. Vărdaru et al. (2022) found that graphene oxide-silicon (GO-Si) HNFs consistently outperformed mono-nanofluids in TC. The 0.8GO: 0.2Si HNF achieved a maximum TC enhancement of 7.97% at elevated temperatures. Additionally, GO/water nanofluids demonstrated superior TC compared to Si/water nanofluids across various concentrations, indicating that adding graphene oxide significantly boosts TC in silicon-based nanofluids.

Kanti et al. (2023a) observed that TC in nanofluids with varying GO and MXene ratios increases with temperature due to enhanced particle interactions. As shown in Figure 3, the TC of different GO/
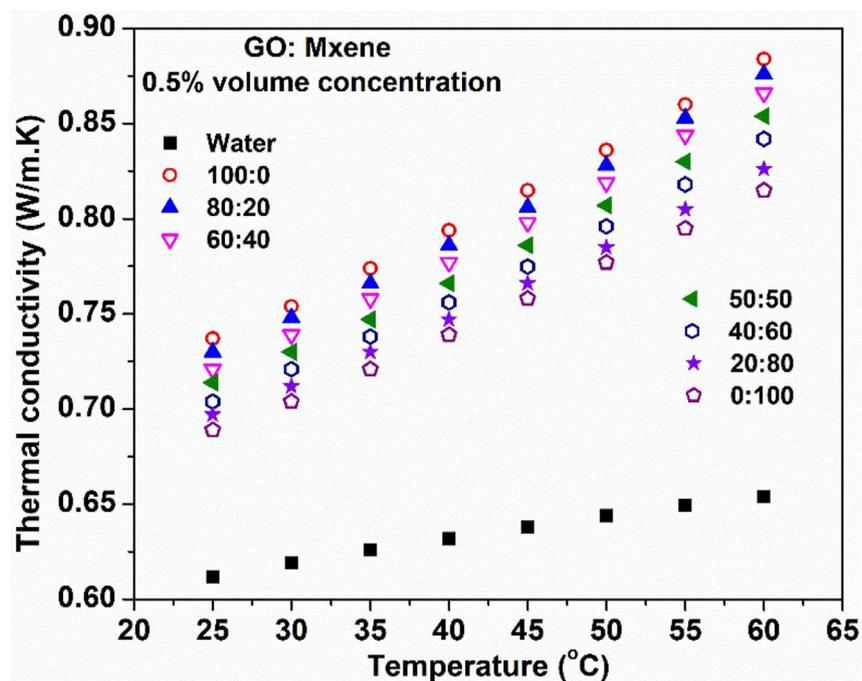
FIGURE 3
Thermal conductivity of different GO/MXene nanofluid mixtures relative to temperature (Kanti et al., 2023a).

MXene nanofluid mixtures increases with rising temperature. At 25°C, TC enhancements for GO, GO-MXene hybrids (80:20 to 20:80), and MXene ranged from 12.6% to 20.4% relative to water, while at 60°C, these values rose to 24.6%–35.2%. Higher GO content in HNFs showed superior TC improvements, which were attributed to GO's better heat conduction and stacking properties. While MXene's solvent compatibility is notable, its lower TC limits its effectiveness. GO-rich HNFs are preferred for thermal applications, particularly in temperature-sensitive systems like solar collectors, though fluid stability and dispersibility need further investigation for practical use.

Alfellag et al. (2024) examined the TC of CT-MWCNTs-TiO$_2$/DW nanofluids and found that TC increased with temperature for all mixing ratios. The highest TC of 0.76 W/m·K was recorded at 50°C for the 60:40 MWCNT-TiO$_2$ ratio, while the lowest, 0.64 W/m·K, occurred at 30°C for the 20:80 ratio. TC improved with increasing MWCNT content up to the 60:40 ratio, after which a slight decrease was observed due to nanoparticle clustering. The study reported a TC enhancement of 18.24% at 50°C for the 60:40 ratio, outperforming mono-nanofluids. This improvement was attributed to the combined heat transfer mechanisms of MWCNTs' efficient conduction along their cylindrical structure and TiO$_2$'s heat scattering.

Tong et al. (2020) investigated the TC of Fe$_3$O$_4$ and MWCNT/Fe$_3$O$_4$ HNFs under varying temperatures and concentrations. Fe$_3$O$_4$ nanofluids showed increasing TC with temperature and nanoparticle concentration, reaching 0.541 W/m·K at 0.2 wt% and 50°C. MWCNT/Fe$_3$O$_4$ HNFs further improved TC, with a maximum of 0.562 W/m·K at a 4:1 MWCNT to Fe$_3$O$_4$ ratio at 50°C. The enhanced heat transfer was attributed to the synergistic effects of MWCNT and Fe$_3$O$_4$, with stable dispersion due to the

strong attachment between particles, forming chainlike structures under a magnetic field, which boosts thermal energy transport. This trend of increased TC with increased concentration of MWCNT was consistent with findings by Balaga et al. (2019) on similar HNFs. Balaga et al. (2019) experimentally measured the TC of f-MWCNT-Fe$_2$O$_3$ HNFs with varying weight ratios of Fe$_2$O$_3$ and f-MWCNT, using deionized water as the base fluid. The study explored weight ratios of 4:1, 3:2, 1:1, 2:3, and 1:4 at concentrations of 0.01%, 0.02%, and 0.03%, over temperatures ranging from 30°C to 60°C. TC increased with a higher MWCNT ratio, peaking at the 2:3 ratio, after which aggregation caused a decline. At 0.02% concentration and 60°C, TC improved by 13.53% compared to 30°C, demonstrating the positive correlation between TC, MWCNT content, and temperature.

In the study by Kumar et al. (2021), the TC performance of HNFs combining multi-walled carbon nanotubes (MWCNTs) with various oxide nanoparticles was analyzed. At a 2 vol% concentration and 50°C, TC ratio (TCR) improvements were 16.53% for Al$_2$O$_3$, 21.44% for TiO$_2$, 27.09% for ZnO, and 33.62% for CeO$_2$, with CeO$_2$ showing the highest enhancement. Even at a lower concentration of 0.25 vol%, MWCNT-based HNFs demonstrated TCR improvements ranging from 6.87% to 16.45%, depending on the oxide used. The study highlighted the synergistic effects of oxide nanoparticles and MWCNT, including Brownian motion, thermal bridging, and particle-liquid interfacial interactions, which collectively enhanced heat transfer properties, resulting in greater TC improvements compared to MWCNT alone.

Selvarajoo et al. (2024) investigated the TC of Al$_2$O$_3$-GO HNFs, finding significant enhancements over mono nanofluids. At a solid volume concentration of 0.25%, the 0.25% Al$_2$O$_3$-GO HNF exhibited a TC of 0.836 W/m·K at 50°C, surpassing the 1.0% Al$_2$O$_3$ mono

nanofluid (0.777 W/m·K) and the 1.0% GO mono nanofluid (0.705 W/m·K). The maximum TC for the 1.0% Al₂O₃-GO HNF reached 0.968 W/m·K at 50°C, indicating a TC enhancement of approximately 24.6% compared to the 1.0% Al₂O₃ mono nanofluid and 37.3% over the 1.0% GO mono nanofluid. These improvements are attributed to the synergistic effects of the two nanoparticle types, which enhance energy transfer within the fluid.

Van Trinh et al. (2018) conducted a detailed study on the TC of ethylene glycol (EG)-based nanofluids with nano additives: hydroxyl-functionalized carbon nanotubes (CNT-OH), carboxylated graphene (Gr-COOH), and a graphene-carbon nanotube (Gr-CNT) hybrid at 0.07 vol%. They found a temperature-dependent increase in TC attributed to enhanced Brownian motion and reduced agglomeration. At 30°C, TC enhancements were 5.2% for CNT-OH, 10% for Gr-COOH, and 18% for Gr-CNT, with Gr-CNT showing nearly 3.5 times greater enhancement than CNT-OH and 2 times greater than Gr-COOH. At 50°C, Gr-CNT achieved a 50% enhancement, compared to 22% for CNT-OH and 37% for Gr-COOH. The results underscore the superior performance of hybrid nanomaterials, with Gr-CNT benefiting from graphene's high TC and carbon nanotubes' strength, making HNFs a promising option for applications requiring enhanced thermal performance in engineering systems.

Despite the consistent improvements observed in TC, there are instances where the advantages of HNFs over single nanofluids are less pronounced. For example, the study conducted by Borode et al. (2021) investigated the TC of GNP-alumina HNFs, revealing that TC increases with temperature for all tested nanofluids, including distilled water. The addition of nanoparticles significantly enhances the TC compared to water alone, with mono-GNP demonstrating higher TC than hybrid formulations. Among the HNFs, a higher proportion of GNP correlates with improved TC performance. Specifically, TC enhancements at varying temperatures are as follows: GNP-alumina (25:75) shows a 1.66%–3.09% increase, GNP-alumina (50:50) 1.99%–4.23%, GNP-alumina (75:25) 1.83%–3.42%, and mono-GNP 4.48%–5.62%. This highlights the superior effectiveness of mono-GNP as a standalone additive for enhancing TC in nanofluids.

Wang et al. (2021) compared the TC of mono nanofluids composed of Fe₃O₄ and CNT, along with HNFs combining both, over a temperature range of 10°C–40°C at a 0.5% volume concentration. Among the mono nanofluids, Fe₃O₄ dispersed with surfactants showed varying TC improvements: Fe₃O₄–TMAH had the highest increase (3.47%–5.43%), followed by Fe₃O₄–TSC (2.48%–4.72%) and Fe₃O₄–Colace (1.47%–4.21%). CNT mono nanofluids exhibited even greater enhancements, with CNT–SDS achieving an 8.23% increase and CNT–GA a 7.54% increase. Overall, CNT-based mono nanofluids outperformed Fe₃O₄ mono nanofluids, particularly with the SDS surfactant. The hybrid Fe₃O₄–CNT nanofluids, especially Fe₃O₄–CNT–SLS, showed improved TC over Fe₃O₄ mono nanofluids, with a 5.78% increase, but still lagged behind CNT mono nanofluids like CNT–SDS and CNT–GA, indicating that while hybridization enhances the TC of Fe₃O₄-based nanofluids, CNT mono nanofluids remain superior in overall performance.

Critically, while many studies report significant improvements in TC, few investigate the broader impact of these enhancements on system-wide performance. For instance, increasing TC may not always translate directly to better overall heat transfer in real-world applications, where factors such as fluid flow, pumping power, and long-term stability play a role. Furthermore, the economic feasibility of scaling up the use of graphene-based hybrids, particularly those incorporating precious metals, remains a challenge. Studies focusing on more cost-effective alternatives to platinum and silver, such as copper or nickel, could provide a pathway to broader adoption.

Importantly, the superior TC of HNFs is not universal across all compositions. Li et al. (2024) investigated the TC of hybrid graphene oxide/silicon dioxide (GO/SiO₂-DW) nanofluids and observed a predictable increase in TC with rising nanoparticle concentration. This aligns with the expectation that higher concentrations enhance TC due to increased particle contact and improved heat transfer pathways. The study also found that TC for both GO and GO-SiO₂ nanofluids increased with temperature, likely due to enhanced Brownian motion and particle interactions. Notably, a direct comparison revealed that GO nanofluids outperformed GO-SiO₂ counterparts at the same concentration and temperature. This suggests that the addition of SiO₂ may hinder the heat transfer capabilities of GO, possibly due to increased interfacial thermal resistance or changes in nanoparticle dispersion. Further investigation into the impact of SiO₂ on the thermal behavior of HNFs would be valuable.

Ahammed et al. (2016) experimentally analyzed the thermal characteristics of alumina, graphene, and HNFs, finding that hybridizing graphene with alumina decreased TC. They reported TC enhancements of 26.92% for graphene, 13.84% for the hybrid, and 8.2% for alumina. This challenges the assumption that hybridization improves TC, as the interaction between graphene and alumina can disrupt thermal synergy due to alumina's lower intrinsic conductivity, leading to reduced heat transfer. Thus, nanoparticle interactions in hybrids may be counterproductive depending on the combination. Thus, in hybrid systems, optimizing the ratio between different nanoparticles is critical. If one nanoparticle acts as a thermal bottleneck, as suggested by alumina's impact on graphene, it could hinder the hybrid's overall effectiveness. These findings emphasize that while HNFs hold promise, achieving consistent TC improvements requires careful design and a thorough understanding of the interactions at play. Table 1 summarizes the key findings on the TC of various carbon-based HNFs.

In summary, while carbon-based HNFs, especially those incorporating graphene or CNTs, show significant potential in enhancing TC, there are critical challenges that must be addressed. These include managing particle agglomeration at higher concentrations, maintaining long-term stability, and balancing cost-effectiveness. Comparisons between single and HNFs consistently demonstrate the superior thermal performance of hybrid systems. Still, future research should focus on mitigating the drawbacks of increased viscosity and stability issues, particularly for practical, large-scale applications.

2.2 Viscosity

While carbon-based HNFs exhibit substantial improvements in TC, these enhancements often come at the cost of increased viscosity, which can negatively impact flow and pumping power

TABLE 1 Summary of the thermal conductivity results of carbon-based HNFs.

Authors	Hybrid nanoparticle	Base fluid	Concentration range	Temperature (°C)	Thermal conductivity results
Kumar et al. (2024)	GO-MXene	Vanadium electrolyte	0–0.1 wt%	15–45	1.57% and 6.81% enhancement for 0.01wt% and 0.1 wt% HNF at 45°C, respectively
Li et al. (2024)	GNPs/Al₂O₃	Oleic Acid	GNPs: 0.1 wt%-0.4 wt%	30	A 10% GNP addition in the Al₂O₃ HNF resulted in the maximum enhancement of 12.84% at 4 wt%
			Al2O₃: 1 wt%-4 wt%		Decrease in TC with increased addition of GNP to 15%
					Mono-GNP NF of 0.4wt% has a maximum enhancement of 9.04%
Kanti et al. (2024)	Red Mud (RM)-GO (50:50)	Water	0.1–0.75 vol%	60	0.75vol% HNF has the highest TC of 0.93 W/m.K at 60°C
					This HNF has a higher TC than mono RM NF of 0.75 vol%
Jin et al. (2024)	GO/MXene (1:1)	Ethylene glycol (EG)/water-based (50:50)	0.01 wt%-0.3 wt%	20–60	TC increased with GO/MXene dosage
					0.3 wt% HNF shows the greatest TC improvement of 33.49% at 60°C
Alsangur et al. (2024)	Fe₃O₄/CNT, Fe₃O₄/Graphene	Water	1–5 wt%	24	The TC of Fe₃O₄/Graphene is up to 2–3 times more than that of Fe₃O₄/CNT
					Under the external magnetic field effect, the maximum TC enhancement results were around 12% and 51% for 5 wt% of Fe₃O₄/CNT-water and Fe₃O₄/Graphene-water, respectively
					Without an external magnetic field, TC enhancement for the HNFs is 6.7% and 14.6% for Fe₃O₄/CNT-water and Fe₃O₄/Graphene-water, respectively. at 5 wt%
Alfellag et al. (2024)	CT-MWCNTs/TiO₂	Water	0–0.1 wt%	30–50	TC increased with an increase in CT-MWCNT proportion from 20:80 to 60:40, and then it experienced a slight decrease for the HNF ratio of 80:20
					HNF 60:40 has the highest augmentation of 18.24% at 50°C
Sreekumar et al. (2024)	MXene/Carbon-dot	Water	0.01–0.2 wt%	20–60	MXene has the highest TC enhancement (50%) over water, followed by hybrid (42.2%) and C-dot nanofluid (33.2%)
Ibrahim et al. (2024)	Al₂O₃-MWCNT	Water	0.3 vol%	10–30	TC is enhanced by about 48.86% at a volume concentration of 0.3
Selvarajoo et al. (2024)	Al₂O₃-GO (80:20)	Deionized water	0.25–1.0 vol%	30–50	4.30% higher HNF TC than Al₂O₃, 4.34% higher than GO
Al-Rabeeah et al. (2024)	Graphene-Fe₃O₄	Water	0.01%–0.2%	20–60	4.87% enhancement for 0.2% HNF at 20°C
Singh et al. (2024)	Graphene-ZrO₂	Water	0.05%–0.125%	30°C–70°C	The TC of the nanofluid is enhanced by 16.87% at 70°C with 0.125% Graphene-ZrO₂ nanofluid
Srinivasan and Ponnusamy (2024)	Oxygen-functionalized GNP-CuO	DI water	0.1 wt%	30–60	The 50:50 ratio of hybrid NFPCM had the highest enhancement: 17.69% (liquid state) and 30.75% (solid-state) compared to the base PCM
Kumar Kanti et al. (2023)	CuO-GO	Water	0.1–1 vol%	30–60	HNFs with a higher proportion of GO demonstrate greater TC enhancement than those with more CuO
					GO mono-NF has the highest augmentation of 52.4% at 60°C for 1 vol%

(Continued on following page)

TABLE 1 (*Continued*) Summary of the thermal conductivity results of carbon-based HNFs.

Authors	Hybrid nanoparticle	Base fluid	Concentration range	Temperature (°C)	Thermal conductivity results
					HNF (50:50) has a 48.3% enhancement at 1 vol% and 60°C
Razavi Dehkordi et al. (2023)	WO$_3$-nG	Liquid Paraffin	0.005%–5%	25–70	Increased with the increment of mass fraction percentage and temperature, optimum value observed at 5% and 70°C
Bao et al. (2023)	MWCNT/SiC	Water	10 ppm MWCNTs, 80 ppm SiC	25	TC is enhanced by 0.43% at 0.1 wt% (10 ppm) of nanoparticles
Kanti et al. (2023a)	GO-MXene	Water	0.5 vol%	25–60	GO mono-NF showed the highest TC enhancement of 35.2% at 60°C
					GO-MXene (80:20) HNF has a 33.9% enhancement at 60°C
					TC enhancement decreased with increasing MXene concentration in the HNF
Vărdaru et al. (2023)	Ag-rGO (50:50)	Water	0.05–0.1 wt%	20–50	10.69% enhancement at 0.1 wt% and 50°C
Kanti et al. (2023b)	GO-Al$_2$O$_3$ (20:80 and 50:50)	Water	0.1–1.0 vol%	30–60	GO NF has a higher TC than the HNFs when compared with water
					GO-Al$_2$O$_3$ HNF with 20:80 and 50:50 ratio has an enhancement of 39.6% and 46.6%, respectively, at 1.0 vol% and 60°C
Kumar Kanti et al. (2023)	GO-CuO	Water	0.1–1.0 vol%	30–60	GO NF has a higher TC than the HNFs when compared with water
					GO-CuO HNF with 20:80 and 50:50 ratio has an enhancement of 41% and 48.3%, respectively, at 1.0 vol% and 60°C
Kanti et al. (2022)	GO-SiO$_2$ GO-TiO$_2$	Water	0.05–1.0 vol%	30–60	Mono GO NF has a higher TC (52.8%) than the HNFs when compared with water
					The HNFs have a TC enhancement of 43.0% and 38.4% for GO-SiO$_2$ and GO-TiO$_2$ HNF at 1.0 vol% and 60°C, respectively
					The addition of GO to TiO$_2$ and SiO$_2$ NF improves its TC
Vărdaru et al. (2022)	GO-Si	Water	0–0.25 wt%	25–50	HNFs with a higher proportion of GO exhibit greater TC enhancement than those with more Si
					0.8 GO- 0.2 Si HNF has the maximum enhancement of 7.97% at 0.25 wt% and 50°C
Kanti and Maiya. (2022)	GO/coal fly ash (CFA)	Water	0.1–1.0 vol%	30–60	GO mono NF has the highest TC increment of 52.4% for 1 vol% at 60°C
					Increased addition of GO in the HNF increases TC
					GO/CFA (50:50) and GO/CFA (30:70) HNF have an increment of 45.6% and 41.3%, respectively, at 60°C for 1.0 vol% relative to the water
Shajan et al. (2021)	Al$_2$O$_3$-GNP	Therminol® 55	0.01–0.1 wt% (GNP), 1.0 wt% (Al$_2$O$_3$)	20–90	Higher HNF TC than mono NF
					10.28% HNF TC enhancement compared to TH55-Al$_2$O$_3$, 3.03% enhancement compared to TH55-GNP
Siddiqui et al. (2021)	Ag-Graphene	Water	0.10%	20–100	2%–8% enhancement for MR-2 SGHF from 20°C to 70°C
Balaji et al. (2021)	Graphene-MWCNT	Water	0.01%–0.2%	20–60	25% enhancement for 0.2%

TABLE 1 (*Continued*) Summary of the thermal conductivity results of carbon-based HNFs.

Authors	Hybrid nanoparticle	Base fluid	Concentration range	Temperature (°C)	Thermal conductivity results
Bakhtiari et al. (2021)	TiO_2-Graphene	Water	0.005%–0.5%	25–75	Graphene mono NF has higher TC than TiO_2 mono NF and the HNF
					The HNF has a TC increase of 27.84% at a volume fraction of 0.5% and 75°C compared to the base fluid
Said et al. (2020)	rGO coated over F-CNF	Water	0.04 vol%	25–55	Enhanced TC of 0.798 W/m.K at 55°C when compared to mono NFs
Kazemi et al. (2020)	Graphene-SiO_2 (70:30)	Water	0.05%–1%	25°C–50°C	Maximum TC enhancement of 36.12% for 1 vol% HNF at 50°C
Moghadam et al. 2020	GO-TiO_2	Water	0.05%–1%	20°C–50°C	The TC of the nanofluid is enhanced by 32.8% at 50°C with a 1% volume fraction
Soltani et al. (2020)	WO_3-MWCNTs	Oil	0.05%–0.6%	20–60	Maximum TC enhancement of 19.5% with HNF of 0.6% and 60°C
Kishore et al. (2020)	Cu-GNPs	Water	0.01%–0.02%	Up to 100	0.02% HNF has the largest TC enhancement of 9.95% in comparison to distilled water
Taherialekouhi et al. (2019)	Graphene Oxide-Al_2O_3	Water	0.1%–1%	25°C–50°C	The TC of the nanofluid increased by 33.9% at 1% volume fraction and 50°C
Rostami et al. (2019)	GO-CuO	EG/Water (50:50)	0.1%–1.6%	25–50	A maximum enhancement of 43.4% was observed at the highest volume fraction
Dalkılıç et al. (2018)	CNT-SiO_2	Water	0.1–1 vol%	25–60	Maximum enhancement of 26.29% was observed in TC.
Van Trinh et al. (2018)	Gr-CNT	Ethylene Glycol	0–0.07 vol%	30–50	The enhancement in TC is 18% and 50% at 30°C and 50°C, respectively
Askari et al. (2017)	Fe_3O_4-Graphene	Water	0–1 wt%	20–40	Maximum TC enhancement of 32% for 1.0 wt% HNF at 40°C
Syam Sundar et al. (2017)	GO-Co_3O_4	Water	0.05%–0.2%	20–60	19.14% enhancement for 0.2% at 60°C
Mehrali et al. (2017)	rGO-Fe_3O_4	Water	0.5 wt%	10–40	TC of rGO–Fe_3O_4 nanofluid enhanced up to 11%
Sarbolookzadeh Harandi et al. (2016)	F-MWCNT – Fe_3O_4	EG	0–2.3 vol%	25–50	Max TC augmentation of 30% for 2.3% HNF at 50°C
Yarmand et al. (2016b)	GNP-Pt	Water	0–0.1 wt%	20–40	The HNF has a 17.77% enhancement at 0.1 wt% and 40°C
Yarmand et al. (2016a)	Activated Carbon - GO	EG	0.02%–0.06%	20–40	The enhancement of TC is 6.47% at 40∘C and a weight fraction of 0.06%
Yarmand et al. (2015)	GNP-Ag	Water	0.02%–0.1%	20–40	For 0.1% weight concentration of GNP-Ag, the enhancement of TC is 16.94% at 20°C and nearly 22.22% at 40°C
Shahsavar et al. (2015)	CNT/Fe_3O_4	Water	0.1–0.9 vol% Fe_3O_4 0–1.35 vol% CNT	25–55	Increasing the proportion of CNT in the HNF enhances TC
					The HNF with 0.9% Fe_3O_4 and 1.35% CNT showed the greatest improvement of 45.41% and 152.95% in TC, respectively, without and with exposure to a 470 mT magnetic field

requirements. For instance, Kishore et al. (2020) investigated copper-graphene HNFs, reporting a 9.95% increase in TC and a 13.83% rise in viscosity. While the TC improvement enhances heat transfer, the higher viscosity can impede fluid mobility in applications requiring high flow rates. This highlights the need to balance thermal and rheological properties, as increased viscosity may lead to greater frictional losses and higher operational costs due

to the necessity for more powerful pumps, posing challenges in optimizing HNFs for practical use. In a study by Said et al. (2021), the enhancement in TC with increasing nanoparticle concentration in water-based Fe_3O_4-coated MWCNT HNFs is counteracted by a significant increase in viscosity. At 0.3% volume concentration, the TC improved by 13.78% and 28.33% at 20°C and 60°C, respectively, compared to water. However, this improvement is offset by a

considerable rise in viscosity, which increased by 27.83% at 20°C and 50% at 60°C. In their 2024 study, Jin et al. (2024) investigated the viscosity of GO/MXene nanofluids, finding that viscosity decreased with increasing temperature, with a notable reduction of 33.33% at 60°C for a 0.3 wt% concentration due to enhanced Brownian motion and larger void sizes between nanoparticles. However, higher concentrations led to slight viscosity increases. At 60°C, viscosity increments relative to the base fluid (EG/water) ranged from 1.49% to 16.42%. While significant TC improvements were noted, the increased viscosity could negatively impact fluid dynamics, emphasizing the need to balance thermal and rheological properties in HNF design to avoid excessive pumping power requirements and efficiency loss.

Selvarajoo et al. (2024) comprehensively examined the thermal properties of Al_2O_3-GO HNFs, focusing on dynamic viscosity and TC at various temperatures and nanoparticle concentrations. They found that increasing temperature significantly reduced the dynamic viscosity of both hybrid and mono nanofluids, with the base fluid viscosity decreasing from 0.82 mPa s to 0.57 mPa s (approximately 30.6%) when the temperature rose from 30°C to 50°C. The 1.0% GO mono nanofluid exhibited the highest viscosity reduction at 11.2%, while the 0.25% Al_2O_3-GO HNF showed a 6.07% decrease. At 30°C, the viscosity of the 0.25% Al_2O_3-GO HNF was 2.69% higher than that of the 1.0% Al_2O_3 and 1.0% GO mono nanofluids. The viscosity difference between the 0.25% and 1.0% concentrations was 0.21 mPa s, or 20.7%, indicating that lower-concentration HNFs tend to have higher viscosities than mono nanofluids.

Syam Sundar et al. (2017) observed a significant increase in TC for graphene oxide and Co_3O_4 HNFs, with a 19.14% rise in water-based and 11.85% in EG-based nanofluids at 0.2% concentration at 60°C. However, the viscosity also increased significantly by 1.7 times in water and 1.42 times in, EG, posing challenges for flow efficiency. This highlights a trade-off in HNFs, where improved heat transfer comes at the cost of higher viscosity, which increases drag forces, pumping costs, and system complexity.

Ilyas et al. (2023) conducted a comparative study on the viscosity of graphene nanofluids and hybrid formulations with carbon nanotubes (G + CNT) and carbon nanofibers (G + CNF). Graphene nanofluids had the lowest viscosity, which increased with concentration, while G + CNT HNFs showed the highest viscosity across all concentrations, with G + CNF falling in between. The higher viscosity of HNFs is attributed to the complex particle interactions and denser network formations that increase flow resistance. The study underscores the importance of balancing viscosity and TC when selecting nanofluids for specific applications.

However, in some cases, HNFs demonstrate lower viscosity compared to their single nanofluid counterparts. For instance, Borode et al. (2021) investigated the viscosity behavior of mono-GNP nanofluids and GNP-alumina HNFs at 25°C. Mono-GNP nanofluids showed a 10.53% viscosity increase compared to distilled water, while GNP-alumina (75:25) HNFs had a lower increase of 9.73%, and GNP-alumina (50:50) HNFs exhibited a further reduced increment of 7.96%. The findings suggest that combining GNP with alumina improves particle dispersion and reduces inter-particle interactions, leading to better flow properties. Thus, HNFs offer improved viscosity characteristics over single

nanofluids, making them suitable for applications requiring thermal efficiency and manageable viscosity.

Ranjbarzadeh et al. (2018) evaluated the viscosity of water/graphene oxide-silicon oxide HNFs and water/graphene oxide nanofluids at concentrations of 0.05%, 0.2%, and 0.8% over temperatures of 20°C, 40°C, and 60°C. The HNF reduced nanoparticle costs while enhancing viscosity compared to the pure graphene oxide nanofluid. This increase was attributed to graphene oxide's plate-like structure, which provides a high surface area and stronger fluid interactions. Silicon oxide's spherical shape, with a lower surface area, balanced the structure, preventing excessive viscosity. These results highlight the benefits of hybrid formulations in optimizing viscosity for different applications.

Kumar and Sarkar (2020) compared the viscosities of mono alumina and hybrid alumina-MWCNT nanofluids, revealing that alumina nanofluids exhibited lower viscosity than hybrid formulations, while mono MWCNT nanofluids had higher viscosity than the hybrid. This is due to the spherical shape of alumina nanoparticles, which promotes better dispersion and lower viscosity. At the same time, MWCNTs' elongated structure increases viscosity due to greater surface area and fluid interaction. For applications prioritizing flow, alumina nanofluids offer lower viscosity, whereas MWCNTs enhance TC despite their higher viscosity, requiring a balanced formulation to meet specific thermal needs.

Kanti et al. (2023b) conducted a rheological study on nanofluids containing GO and MXene to assess their viscosity behavior. The nanofluids exhibited Newtonian characteristics, with viscosity largely independent of shear rate, making them suitable for consistent heat transfer applications. Figure 4 illustrates the effect of temperature on the dynamic viscosity of various GO/MXene nanofluid mixtures. Viscosity decreased with increasing temperature due to reduced intermolecular forces and increased nanoparticle mobility. At 25°C, viscosity enhancements relative to water were 110.1% for GO, 96.6% for GO-MXene (80:20), and 21.3% for MXene, with lower enhancements at 60°C. GO-based nanofluids showed the highest viscosity, while MXene reduced viscosity, likely due to its smoother edges acting as lubricants, offering an optimal balance between TC and manageable viscosity.

Borode et al. (2024) found that the viscosity of HNFs decreases with an increase in the mixing percentage of GNP. The study showed that hybridizing Fe_2O_3 nanofluid with GNP results in a reduction of viscosity. This reduction occurs because GNP acts as spacers between Fe_2O_3 nanoparticles, preventing their aggregation and enhancing the fluidity of the nanofluid. The size and shape of GNP, which allow it to move more freely in the base fluid, further contribute to the decrease in viscosity. This synergistic effect between Fe_2O_3 and GNP leads to improved fluid dynamics in the HNF.

Shajan et al. (2021) examined the viscosity behavior of various nanofluids, including Al_2O_3 and GNP, as well as their hybrid formulations. They found that viscosity decreases with increasing temperature for both mono and hybrid nanofluids, with a reduction of 91.17%–84.5% as the temperature rose from 20°C to 90°C. However, higher nanoparticle concentrations increased dynamic viscosity due to enhanced Van der Waals interactions between fluid molecules and nanoparticles. GNP mono-nanofluids
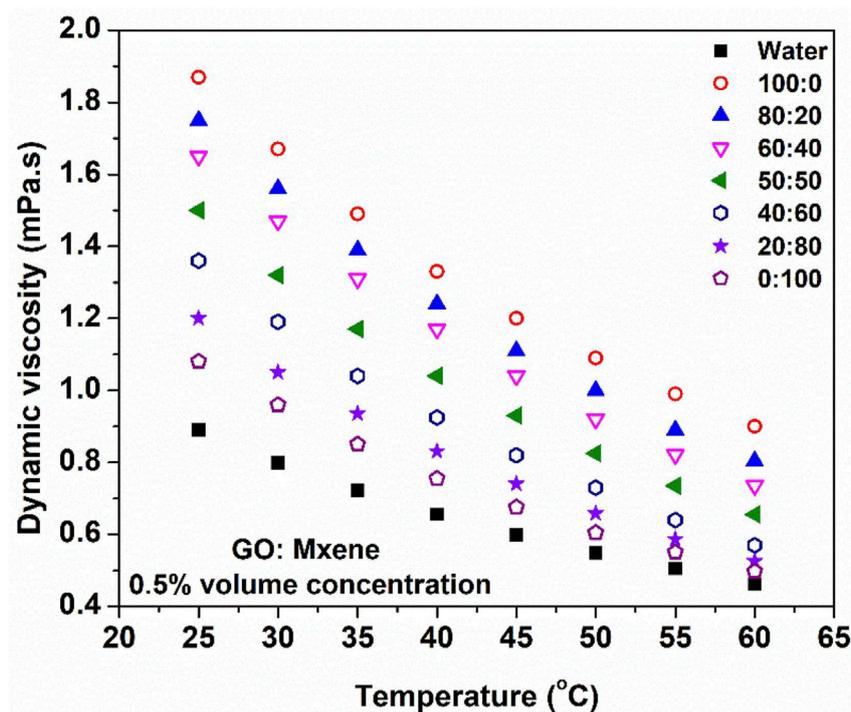
FIGURE 4
Viscosity of different GO/MXene nanofluid mixtures relative to temperature (Kanti et al., 2023b).

exhibited higher viscosity than Al_2O_3, indicating that excessive GNP concentrations could be detrimental, leading to higher pressure drops and pumping power requirements. The relative viscosity of the HNF(TH55-GNP/Al_2O_3) was notably higher at elevated temperatures, possibly due to particle clustering or increased Brownian motion, showing a viscosity enhancement of 66.69% compared to pure TH55 oil at 20°C, significantly surpassing the increases seen in mono-nanofluids.

Alfellag et al. (2024) investigated the effects of mixing ratios and temperature on the viscosity of CT-MWCNTs-TiO_2/DW HNFs. They found that viscosity decreases with increasing temperature, with the highest viscosity of 0.87 mPa s at 30°C for the 80:20 mixing ratio and the lowest of 0.645 mPa s at 50 °C for the 20:80 ratio. Increasing the MWCNT content in the mixing ratio led to higher viscosity due to the formation of network structures that hinder flow, as MWCNTs have a higher aspect ratio compared to spherical TiO_2 particles. The single CT-MWCNTs/DW nanofluids exhibited a 30.9% viscosity increase at 50°C, attributed to the cylindrical shape of MWCNTs, while TiO_2/DW nanofluids showed the lowest increase of 4.2% at 30 °C. Moderate increases in viscosity were observed in HNFs with rising temperature and mixing ratio, particularly in the 80:20 ratio due to the higher MWCNT content.

These observations indicate that the choice of single particles in HNFs is critical as it directly influences the resulting thermophysical properties. The combination of different nanoparticles can lead to synergistic effects, potentially enhancing TC beyond what is achievable with single nanofluids. However, it's also evident that these synergistic effects are not guaranteed, and the specific combination and proportion of nanoparticles can significantly impact the final properties. Also, exceeding certain concentration thresholds or using non-optimal mixing ratios can lead to detrimental effects, such as increased viscosity or decreased TC, highlighting the importance of careful selection and optimization of nanoparticle combinations in HNFs. Table 2 summarizes the key findings on the viscosity of various carbon-based HNFs.

In conclusion, while carbon-based HNFs offer substantial TC enhancements, their increased viscosity poses a significant challenge. Many studies show that HNFs typically suffer from higher viscosity compared to single-component nanofluids, which can reduce their effectiveness in systems where fluid mobility is crucial. Future research should focus on finding ways to mitigate viscosity increases, such as through nanoparticle surface modification, the use of advanced stabilizers, or optimizing nanoparticle concentrations. Furthermore, long-term studies are needed to explore the stability of these fluids under varying operational conditions, particularly in systems where temperature, shear stress, and fluid flow rates fluctuate.

2.3 Specific heat capacity

Specific heat capacity (Cp) is a key thermophysical property that influences the ability of a nanofluid to store and transfer thermal energy. In the case of carbon-based HNFs, the addition of nanoparticles typically results in a decrease in SHC compared to the base fluid, as the solid particles generally have lower specific heat than the fluid. This reduction can offset some of the benefits gained from enhanced TC, as it limits the fluid's ability to absorb and store heat. For instance, Yarmand et al. (2016b) investigated the SHC of GNP-Pt HNFs. They found that the SHC decreased by 6.26% at a

TABLE 2 Summary of the viscosity results of carbon-based HNFs.

Authors	Hybrid nanoparticle	Base fluid	Concentration range	Temperature (°C)	Viscosity results
Kumar et al. (2024)	GO-MXene (90:10)	Vanadium electrolyte	0–0.1 wt%	15–45	14.5% and 10% increase for 0.1 wt% HNF at 15°C and 45°C, respectively
Alfellag et al. (2024)	CT-MWCNTs/TiO$_2$	Water	0–0.1 wt%	30–50	Increasing the CT-MWCNT proportion in the HNF gradually increased the dynamic viscosity of the hybrid nanofluid
					The highest viscosity of 0.87 mPa s was observed for the mixing ratio of 80:20 at 30°C, while the lowest value of 0.645 mPa s was recorded for the 20:80 mixing ratio at 50°C
Huminic et al. (2024)	Ag NPs-rGO	Water/Ethylene Glycol	0.050–0.10 wt%	20–50	The maximum increase in viscosity was 2.33 times (approx. 24%) at 293.15 K and 0.10 wt%
Kanti et al. (2024)	RM-GO (50:50)	Water	0.1–0.75 vol%	60	Increased with increasing hybrid NP concentration
					0.75vol% HNF has the highest viscosity of 0.728 mPa.S at 60°C
					Mono RM NF of 0.75 vol% has the lowest viscosity compared to all the HNFs
Jin et al. (2024)	GO/MXene (1:1)	Ethylene glycol (EG)/water-based (50:50)	0.01 wt%-0.3 wt%	20–60	Viscosity slightly increased with GO/MXene dosage
					0.3 wt% HNF shows the greatest TC improvement of 16.42% at 20°C
Selvarajoo et al. (2024)	Al$_2$O$_3$-GO (80:20)	Deionized water	0.25–1.0 vol%	30–50	4.6% reduction compared to deionized water
Al-Rabeeah et al. (2024)	Graphene-Fe$_3$O$_4$	Water	0.01%–0.2%	20–60	59% decrement for 0.2% HNF from 20°C to 60°C
Srinivasan and Ponnusamy (2024)	Oxygen-functionalized GNP-CuO	DI water	0.1 wt%	20	Hybrid NFPCMs, especially with higher CuO ratios, showed greater viscosity enhancement
					O$^+$f-GNPs – CUO (25:75) HNF-PCM has the highest viscosity increase of 15.2% at 20°C
					Mono O$^+$f-GNPs have a lower viscosity increment than single CuO NFs and HNFs
Li et al. (2024)	GNPs/Al2O$_3$	Oleic Acid	GNPs: 0.1 wt%-0.4 wt%	30	The viscosity of the nanofluid increases as the concentration and the proportion of GNPs increase from 0%–10%
			Al2O$_3$: 1 wt%-4 wt%		An increase of 10%–15% reduces the viscosity due to poor dispersion
Vărdaru et al. (2023)	Ag-rGO	Water	0.05%–0.1 wt%	20°C–50°C	The viscosity of Ag-rGO/water hybrid nanofluids increased by approximately 13% with 0.1 wt% and at 50°C
					17.38% maximum increase at 0.1 wt% and 20°C
Kanti et al. (2023b)	GO-Al$_2$O$_3$	Water	0.1–1.0 vol%	30–60	Mono GO NF has a higher viscosity increment than the HNFs, while that of Al$_2$O$_3$ NF is lesser
					47.5% and 101% viscosity increase at 1.0 vol% and 30°C for 20:80 and 50:50 HNFs, respectively
Kumar Kanti et al. (2023)	CuO-GO	Water	0.1–1 vol%	30–60	GO mono-NF has the highest viscosity increment of 177% at 30°C for 1 vol%
					HNFs with a higher proportion of GO exhibit greater viscosity enhancement than those with more CuO

TABLE 2 (*Continued*) Summary of the viscosity results of carbon-based HNFs.

Authors	Hybrid nanoparticle	Base fluid	Concentration range	Temperature (°C)	Viscosity results
					HNF (50:50) and (20:80) have a 115.3% and 55.2% increase at 1 vol% and 30°C, respectively
Kanti et al. (2023a)	GO-MXene	Water	0.5 vol%	25–60	GO mono-NF showed the highest viscosity enhancement of 110.1% at 25°C and 94.8% at 60°C
					96.6% increase for GO-MXene (80:20) HNF at 25°C viscosity enhancement decreased with increasing MXene concentration in the HNF
Kanti and Maiya (2022)	GO/coal fly ash (CFA)	Water	0.1–1.0 vol%	30–60	GO mono NF has the highest viscosity increment of 177% for 1 vol% at 30°C
					Adding CFA to GO NF reduces the HNF viscosity
					GO/CFA (50:50) and GO/CFA (30:70) HNF have an increment of 152% and 113%, respectively, at 30°C for 1.0 vol% relative to the water
Kanti et al. (2022)	GO-SiO$_2$	Water	0.05–1.0 vol% (50:50)	30–60	Mono GO NF has a higher viscosity increment (175%) than the HNFs, while those of mono TiO$_2$ and SiO$_2$ NFs are lesser
	GO-TiO$_2$				HNFs show a maximum viscosity increment of 130.3% and 144% for GO-SiO$_2$ and GO-TiO$_2$ HNF at 1.0 vol% and 30°C, respectively
Shajan et al. (2021)	Al$_2$O$_3$-GNP	Therminol® 55	0.01–0.1 wt% (GNP), 1.0 wt% (Al$_2$O$_3$)	20–90	66.69% maximum increase found for the viscosity of 0.1 wt% GNP- 1.0% Al$_2$O$_3$ HNF at 20°C
Kishore et al. (2020)	Cu-GNPs	Water	0.01%–0.02%	Up to 100	The viscosity of 0.02% hybrid nanofluid is enhanced by 13.5% in comparison to the distilled water
Said et al. (2020)	rGO coated over F-CNF	Water	0.04 vol%	25–55	Mono NFs have a higher viscosity than the HNF
					At 20°C and 0.02 vol%, the viscosity increased by over 15.2% (CNF), 12.5% (F-CNF), 7.2% (rGO), and 6.3% (F-CNF/rGO)
Kazemi et al. (2020)	Graphene-SiO$_2$	Water	0.05%–1%	25°C–50°C	The viscosity of the hybrid nanofluids is between the viscosity of mono nanofluids, while Graphene/Water mono-nanofluid samples have the highest value The G–SiO$_2$ (30%–70%)/Water hybrid nanofluid has a higher viscosity than SiO$_2$/Water mono-nanofluid
Syam Sundar et al. (2017)	GO-Co$_3$O$_4$	Water	0.05%–0.2%	20–60	1.70-times enhancement for 0.2% at 60°C
Yarmand et al. (2016a)	GNP-Pt	Water	0–0.1 wt%	20–40	The HNF has a 33% increase at 0.1 wt% and 40°C
Yarmand et al. (2016a)	ACG	EG	0.02%–0.06%	20–40	The viscosity increases nonlinearly with an increase in ACG weight concentration
					0.06 wt% HNF has the highest increment of 4.16%
Yarmand et al. (2015)	GNP-Ag	Water	0.02%–0.1%	20–40	Viscosity increases by about 30% for 0.1% weight concentration of nanofluids compared to the viscosity of the base fluid at 40°C

concentration of 0.1 wt% compared to the base fluid. While the decrease was not drastic, it highlighted a common challenge in using HNFs—the trade-off between enhancing TC and maintaining heat storage capacity. The decrease in specific heat may affect the efficiency of systems that require high energy storage capabilities, such as solar thermal systems or thermal energy storage units.

Huminic et al. (2024) found that the specific heat of Ag NPs-rGO/W + EG HNFs decreases with increasing nanoparticle concentration but rises with temperature. At 293.15 K, specific heat dropped by 5.97%, 6.57%, and 6.94% for concentrations of 0.05%, 0.075%, and 0.10%, respectively. Similar reductions occurred at 323.15 K, with reductions of 5.70%, 6.11%, and 6.54%. Said et al. (2021) reported a similar trend for Fe_3O_4-coated MWCNT nanofluids, where specific heat increased with temperature but decreased at higher nanoparticle volumes, with a 0.55% drop at 0.6 vol%. These trends are consistent across studies.

Kanti et al. (2023a) compared the SHC of mono NFs and HNFs, finding that HNFs, combining GO and MXene, offer better SHC performance than mono NFs. At 25°C, GO has an SHC of 3750 J/kg.K, while MXene is higher at 3946 J/kg.K. The GO-MXene (50:50) hybrid reaches 3814 J/kg.K, demonstrating an intermediate but rising trend with increased MXene content. At 60°C, SHC values follow the same pattern, with GO at 3832 J/kg.K, MXene at 4085 J/kg.K, and the hybrid at 3955 J/kg.K. This synergy, attributed to enhanced fluid molecule vibration and surface energy from MXene, makes HNFs more effective for heat absorption, especially at higher temperatures.

Gao et al. (2021) found that increasing the nanoparticle mass fraction reduced the SHC of GO-Al_2O_3 HNFs, with decreases of 4% and 7% at 0.05 wt% and 0.15 wt% at 20°C, respectively. At 70°C, reductions were smaller (1% and 0.5%), indicating that temperature had a more significant impact on SHC than nanoparticle concentration. HNFs with a 1:1 ratio of Al_2O_3 and GO showed a 1.33% higher SHC than single nanofluids at 20°C due to the complementary properties of the nanoparticles. Similarly, Shajan et al. (2021) observed that the SHC of TH55-based mono and hybrid nanofluids decreased with higher nanoparticle concentrations and temperatures. At 100°C, alumina (1.0 wt%) and GNP (0.1 wt%) mono-nanofluids exhibited SHC reductions of 2.18% and 3.83%, respectively, with GNP having a stronger effect due to its higher TC. For HNFs, GNP concentrations of 0.01, 0.05, and 0.1 wt% resulted in SHC reductions of 3.25%, 4.86%, and 6.11% at 100°C, highlighting the nanoparticles' role in enhancing heat transfer.

Tiwari et al. (2023) studied the effects of temperature, nanoparticle size, and concentration on the SHC of three HNFs: CuO + MWCNT, MgO + MWCNT, and SnO_2+MWCNT, each in a water base. The results indicated that increasing nanoparticle concentration decreases SHC, as nanoparticles generally have lower SHC than deionized water. However, SHC increases with temperature due to enhanced thermal vibrations. For instance, the CuO + MWCNT HNF showed reduced SHC as the volume fraction increased from 0.25% to 1.50%, while SHC rose with temperature from 25°C to 50°C. Smaller nanoparticles (20 nm) resulted in a greater decrease in SHC compared to larger ones (50 nm) due to surface phonon softening. At 1.50% concentration, SnO_2+MWCNT exhibited the greatest SHC reduction (13.23%), followed by CuO + MWCNT (12.84%) and MgO + MWCNT (15.09%).

Critically, while many studies highlight the decrease in SHC with the introduction of carbon-based hybrid nanoparticles, only a few address how this impacts the overall efficiency of heat transfer systems in real-world applications. Notably, while reduced SHC may not significantly affect systems designed purely for rapid heat dissipation, such as cooling systems in electronics, it could hinder performance in thermal energy storage applications. Systems like solar thermal collectors, which depend on high heat storage to capture and store solar energy for extended periods, could see reduced efficiency when using HNFs with lower specific heat capacities.

In conclusion, while carbon-based HNFs generally exhibit lower specific heat capacities than their base fluids, the extent of this reduction varies depending on the type of nanoparticles used and their concentration. HNFs offer superior TC, but their reduced heat storage capacity may limit their effectiveness in certain applications. Future research should focus on optimizing the balance between TC and specific heat, potentially through the use of non-metallic additives or advanced nanoparticle surface treatments. Moreover, it is essential to evaluate the long-term performance of these fluids in real-world conditions, especially in systems where both heat transfer and storage are critical.

2.4 Density

Density is a critical thermophysical property of nanofluids, affecting their performance in heat transfer systems. The introduction of carbon-based hybrid nanoparticles typically increases the nanofluid's density due to the nanoparticles' higher density than the base fluid. This increase can impact essential performance aspects such as pumping power, pressure drop, and energy efficiency, especially in applications requiring fluid circulation.

Early research by Yarmand et al. (2015) observed a slight linear increase in the density of distilled water with added nanoparticles, showing a 0.09% increase at a 0.1% nanoparticle fraction and 40°C. Although minimal, this rise can affect mass flow rates in heat transfer systems and may lead to increased energy consumption in pressure-dependent circulation systems. Huminic et al. (2024) found that adding Ag NPs and rGO to water-ethylene glycol mixtures increased density by 5.58%–5.98% for concentrations of 0.05%–0.10%. Similarly, Said et al. (2021) reported a density increase of 4.56%–4.84% at 0.6 vol%.

While increased TC is a primary focus of nanofluid research, the density increase associated with hybrid nanoparticles presents challenges in practical applications. Higher density affects fluid dynamics and raises the energy needed for circulation, leading to higher operational costs. Syam Sundar et al. (2017) noted that the increased density in graphene oxide-Co_3O_4 HNFs resulted in a more significant pressure drop, requiring additional energy for fluid flow.

Despite these challenges, the increased density can benefit applications requiring higher mass flow rates for enhanced heat transfer, potentially improving the heat transfer coefficient. However, higher density can be limiting in systems needing low pressure and minimal pumping power. Future research should optimize nanoparticle combinations and concentrations to reduce density increases while maximizing thermal performance.

In conclusion, while the increased density of carbon-based HNFs presents challenges, it also offers opportunities. Balancing TC improvements with manageable fluid dynamics is crucial. Future studies should explore methods to mitigate density impacts, such as using less dense materials, novel nanoparticle shapes, or optimized concentrations, to maximize the potential of HNFs in industrial heat transfer applications.

3 Heat transfer application of carbon-based HNF in solar thermal systems

3.1 Flat plate solar collectors

Flat plate solar collectors are a simple and common way to harness the sun's energy. They use a dark, flat surface to absorb sunlight and transfer the heat to a fluid, typically water, flowing through tubes within the collector. This heated fluid can be used for various purposes, such as domestic hot water or space heating. Figure 5 illustrates the components and structure of a typical flat-plate solar collector.

The quest for improved thermal efficiency in FPSCs has spurred extensive research into utilizing HNFs, which combine multiple types of nanoparticles to optimize heat transfer properties. These advanced fluids are increasingly recognized for their ability to enhance thermal performance compared to conventional heat transfer fluids. Hussein et al. (2020) investigated the thermal performance of an FPSC using a water-based HNF formulated with functionalized MWCNT (CF-MWCNTs), functionalized GNPs (CF-GNPs), and hexagonal boron nitride (h-BN) nanoparticles. The nanoparticle concentrations were varied at 0.05 wt%, 0.08 wt%, and 0.1 wt%, with experiments conducted across a temperature range of 20°C–60°C. The results revealed that the 0.1 wt% HNF demonstrated the highest TC, increasing by 64% at 60°C compared to water. At this concentration, the HNF also achieved the highest thermal efficiency, peaking at 85% at a flow rate of 4 L/min, representing a 20% improvement over the base fluid. The study concluded that using the HNF significantly improved the performance of the solar collector, highlighting its potential for solar thermal applications.

Ahmed et al. (2022) examined the influence of a water-based HNF on the thermal efficiency of a FPSC. The HNF was composed of chemically functionalized carbon nanotubes (CF-CNTs) and hexagonal boron nitride (hBN) nanoparticles in a 40:60 ratio. The study evaluated nanoparticle weight concentrations of 0.05 wt%, 0.08 wt%, and 0.1 wt% across a temperature range of 20°C–60°C to determine the thermal performance. The results indicated that the 0.1 wt% HNF achieved the highest TC, with a 34.36% improvement at 60°C compared to distilled water. Furthermore, the FPSC reached its maximum thermal efficiency of 87% when utilizing the 0.1 wt% HNF at a flow rate of 4 L/min. The study concluded that this HNF offers considerable potential as a working fluid for FPSC applications, providing notable improvements in thermal efficiency.

Verma et al. (2018) studied the effects of HNFs on FPSC performance using HNFs made of CuO and MgO nanoparticles combined with MWCNTs in a water base at an 80:20 weight ratio. The nanoparticle volume concentration ranged from 0.25% to 2.0%,

and flow rates varied from 0.5 to 2.0 L per minute. Results indicated that increased nanoparticle concentration enhanced TC and raised fluid viscosity. The optimal conditions were a particle concentration of 0.75%–1.0% and a mass flow rate of 0.025–0.03 kg/s, resulting in exergy and energy efficiencies of 71.54% and 70.55% for the MgO HNF and 70.63% and 69.11% for the CuO HNF, with the MgO HNF showing superior performance.

Lee et al. (2020) studied the performance of water and a binary nanofluid made from MWCNTs and Fe_3O_4 ferrofluid nanoparticles in a flat plate and vacuum tube solar collectors. They tested various mixing ratios at mass fluxes of 420 kg/s·m² and 598 kg/s·m². Figure 6 shows the efficiency of two different solar collectors changes at various HNF concentrations and mass fluxes. The optimal mixture, containing 0.005 vol.% MWCNT and 0.01 vol.% Fe_3O_4, improved FPSC efficiency by 17.6% compared to water and 24.9% in vacuum tube collectors. Increasing mass flux from 420 to 598 kg/s·m² further enhanced efficiency by 7.8% for FPSCs and 8.3% for vacuum tubes. The study concluded that the binary nanofluid significantly enhances solar collector performance, especially in vacuum tube systems.

Lee et al. (2021) investigated various nanofluids in FPSC, VUSC, and HPSC solar collectors, testing single nanofluids (Al_2O_3, SiO_2, CuO, MWCNT, and Fe_3O_4) and binary nanofluids (MWCNT/CuO and MWCNT/Fe_3O_4) at 0.06, 0.08, and 0.1 vol% concentrations with a constant mass flow rate of 0.047 kg/s. MWCNT showed the highest efficiency across all collectors. The FPSC had the smallest error margin compared to experimental data, while the HPSC had the largest. Binary nanofluids improved collector efficiency significantly, with enhancements of 2%–50% for FPSCs, 3%–7% for VUSCs, and 2%–4% for HPSCs, with MWCNT/CuO outperforming MWCNT/ Fe_3O_4. Higher concentrations correlated with increased efficiencies. The study concluded that binary nanofluids, especially MWCNT/ CuO, are more effective for enhancing solar collector efficiency than single nanofluids.

Henein and Abdel-Rehim (2022) studied the impact of MgO/ MWCNT HNF on the thermal performance of ETSCs, using weight ratios of MgO to MWCNTs (80:20, 70:30, 60:40, and 50:50) at a constant concentration of 0.02% and flow rates of 1, 2, and 3 L/min. Results showed that energy and exergy efficiencies improved with higher MWCNT ratios and flow rates, with a maximum energy efficiency increase of 55.83% and exergy efficiency rise of 77.14% at the 50:50 ratio. Increasing MWCNT content from 20% to 30% significantly enhanced collector efficiency. The study concluded that the MgO/MWCNT (50:50) HNF outperformed other combinations, highlighting its potential to enhance ETSC efficiency and advance solar thermal technologies.

Saleh and Sundar (2021) examined the performance of HNFs made from MWCNTs and Fe_3O_4 in a solar flat plate collector with thermosyphon circulation. Conducting experiments at flow rates of 0.1–0.75 L/min and HNF concentrations of 0.05%–0.3%, they observed a 28.46% increase in TC at 0.3% concentration and 60 °C compared to pure water. Viscosity rose by 50.4%, affecting flow behavior, while the Nusselt number improved by 18.68% and the heat transfer coefficient by 39.22%. The friction factor increased by 18.91%, indicating higher flow resistance, and collector thermal efficiency improved by 28.09% at 0.3% concentration. This study highlights the potential of MWCNTs and Fe_3O_4 HNFs to enhance solar flat plate collector performance.

FIGURE 5
Components and structure of a typical flat plate solar collector (Hawwash et al., 2018).
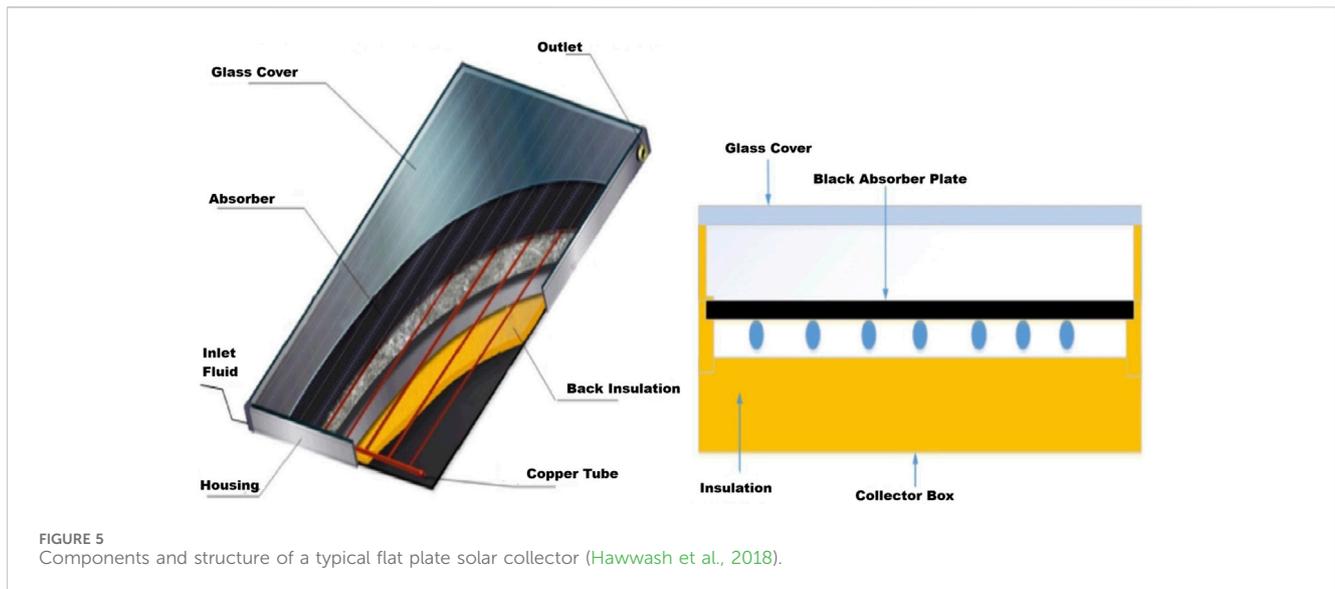
While numerous studies have demonstrated significant enhancements in thermal efficiency through the use of HNFs in FPSC, Huq et al. (2023) examined the stability and thermal performance of a HNF combining GNP and GO at various mass ratios (10:0, 7:1, 6:2, 4:4, and 0:10) while maintaining a total concentration of 0.1 wt%. The 4:4 GNP to GO ratio exhibited the best stability, retaining over 90% concentration after 1 month in static conditions but only 66% after 5 days in actual FPSC flow. Despite this stability, none of the HNFs significantly improved thermal efficiency compared to water. The study concluded that the tested HNFs were unsuitable for the FPSC design used, highlighting the importance of tailoring nanofluid formulations to specific solar collector configurations.

Moreover, a host of studies have highlighted the promising potential of employing HNFs in conjunction with innovative turbulators to improve the thermal performance of FPSC significantly. Negeed et al. (2023) investigated the performance of a FPSC using HNF made of Cu and GO in water, with nanoparticle volume fractions from 1% to 4%. They also employed a turbulator with varying geometric shapes and pitch ratios (γ) from 0.5 to 2. The turbulator significantly enhanced the average Nusselt number (Nuave) and heat transfer performance, particularly at higher Reynolds numbers and nanoparticle concentrations, despite increasing pressure drop (Δp). Energy efficiency improved with Reynolds number and concentration, while exergy efficiency rose with Reynolds numbers but decreased at higher pitch ratios. The study concluded that the HNF and turbulator combination enhances the thermal-hydraulic performance and exergy efficiency of FPSCs, showing potential for solar thermal applications.

Ibrahim et al. (2022) examined the impact of twisted turbulators on the energy and exergy efficiencies and hydraulic performance of solar collectors using single-walled carbon nanotube-copper (SWCNT-Cu) HNFs in water, with concentrations of 1%–3%. They found that the average Nusselt number (Nu) increased with Reynolds numbers (Re) and volume fractions (ϕ). A twisted turbulator with a pitch ratio (PR) of 4 enhanced Nu by 74.95%

at a 3% volume fraction and Re of 36,000. Thermal hydraulic performance (THP) remained above 1, indicating significant improvements. Energy efficiency rose by 41.75% with a PR of 4 at Re from 7,000 to 28,000, while exergy efficiency improved by 33.09% with a PR of 1 at Re from 9,000 to 36,000, demonstrating the effectiveness of twisted turbulators and HNFs in enhancing solar thermal performance.

Ibrahim et al. (2021) studied two-phase water-Al$_2$O$_3$-MWCNT HNFs with 30% MWCNTs and 70% Al$_2$O$_3$ at 1%–3% concentrations. Exergy efficiency increased with Re and volume fractions, with the lowest efficiency at Re of 5,000 and 0.01 volume fraction. At Re of 20,000 and a 0.03 volume fraction, increasing turbulator height from 5 mm to 20 mm reduced exergy efficiency by 16.04%. In a collector with a 5 mm turbulator height and a torsion ratio of 0.25, exergy efficiency decreased by 7.63% compared to a ratio of 0.05. These results underscore the need to optimize turbulator design for improved exergy efficiency in solar collectors using HNFs.

Khetib et al. (2022) investigated innovative turbulator geometries (TIG) combined with DWCNTs and TiO$_2$ in water-based HNFs at concentrations of 1%–3%. Results showed a significant increase in the average Nusselt number (Nu$_{ave}$) with higher Re and volume fractions (ϕ). At Re of 28,000% and 3% volume fraction, TIG with a pressure ratio of 4 led to a 63.46% increase in Nu$_{ave}$. Performance evaluation criteria (PEC) exceeded 1, indicating enhanced performance. Energy efficiency improved by 22.19% as Re rose from 7,000 to 28,000 at pressure ratio of 4, while exergy efficiency improved by 23.26% under similar conditions with pressure ratio of 1, highlighting the potential of innovative turbulator geometries and HNFs in solar collector applications.

Nabi et al. (2022) studied heat transfer enhancement in FPSCs using turbulence-inducing elements and HNFs with SWCNTs and CuO or MWCNTs and CuO at concentrations of 1%–5%. The turbulence elements significantly increased the heat transfer coefficient (HTC) due to improved mixing and contact area with the collector. The third configuration achieved the highest HTC, with increases of about 31% across Reynolds numbers (Re) from

TABLE 3 Summary of Key findings on the performance of carbon-based HNFs in FPSC.

Authors	Hybrid nanoparticle	Base fluid	Concentration range	Findings
Hussein et al. (2020)	f-MWCNTs, f-GNPs, h-BN	Water	0.05 wt%, 0.08 wt%, 0.1 wt%	• 0.1 wt% HNF increased TC by 64% at 60°C
				• thermal efficiency peaked at 85% at 4 L/min flow rate (20% improvement over base fluid)
Ahmed et al. (2022)	CF-CNTs, hBN (40:60 ratio)	Water	0.05 wt%, 0.08 wt%, 0.1 wt%	• 0.1 wt% HNF improved TC by 34.36% at 60°C
				• maximum thermal efficiency of 87% at 4 L/min flow rate
Verma et al. (2018)	CuO/MWCNTs (80:20), MgO/MWCNTs (80:20)	Water	0.25–2.0 vol%	• Increased nanoparticle concentration enhanced TC and viscosity
				• optimal conditions: 0.75%–1.0% concentration, 0.025–0.03 kg/s flow rate, resulting in exergy and energy efficiencies of 71.54% and 70.55% for MgO HNF, and 70.63% and 69.11% for CuO HNF.
Lee et al. (2020)	MWCNTs, Fe_3O_4	Water	0.005 vol% MWCNT, 0.01 vol% Fe_3O_4	• Optimal mixture improved FPSC efficiency by 17.6% compared to water
				• increasing mass flux from 420 to 598 kg/s·m² further enhanced efficiency by 7.8%
Lee et al. (2021)	MWCNT/CuO, MWCNT/Fe_3O_4	Water	0.06, 0.08, 0.1 vol%	• MWCNT showed the highest efficiency; binary nanofluids improved collector efficiency by 2%–50%
				• MWCNT/CuO outperformed MWCNT/Fe_3O_4
Henein and Abdel-Rehim (2022)	MgO/MWCNTs (various ratios)	Water	0.02 wt%	• Energy and exergy efficiencies improved with higher MWCNT ratios and flow rates; MgO/MWCNT (50:50) HNF showed the best performance
				• The enhancement in the energy and exergy efficiencies of the collector is 55.83% and 77.14%, respectively, for MgO/MWCNT (50:50) hybrid nanofluid
Saleh and Sundar (2021)	MWCNTs, Fe_3O_4	Water	0.05%–0.3%	• 28.46% increase in TC at 0.3% concentration and 60°C; viscosity increased by 50.4%; Nusselt number improved by 18.68%
				• The heat transfer coefficient improved by 39.22%, the friction factor increased by 18.91%, and the collector thermal efficiency enhanced by 28.09% at 0.3% concentration
Huq et al. (2023)	GNP, GO (various ratios)	Water	0.1 wt% total	• 4:4 GNP to GO ratio exhibited the best stability; none of the HNFs significantly improved thermal efficiency
Negeed et al. (2023)	Cu, GO	Water	1–4 vol%	• Turbulator enhanced Nu_{ave} and heat transfer; energy efficiency improved with Reynolds number and concentration; exergy efficiency increased with Reynolds numbers but decreased at higher pitch ratios
Ibrahim et al. (2022)	SWCNT-Cu	Water	1–3 vol%	• Nu increased with Re and φ; twisted turbulator with PR of 4 enhanced Nu by 74.95%
				• energy efficiency increased by 41.75%; exergy efficiency improved by 33.09%
Ibrahim et al. (2021)	Al_2O_3-MWCNT (70:30)	Water	1–3 vol%	• Exergy efficiency increased with Re and volume fractions
				• turbulator height and torsion ratio impacted exergy efficiency
Khetib et al. (2022)	DWCNTs, TiO_2	Water	1–3 vol%	• Nu_{ave} increased with Re and φ; TIG with PR of 4 increased Nu_{ave} by 63.46%
				• energy efficiency improved by 22.19%; exergy efficiency enhanced by 23.26%
Nabi et al. (2022)	SWCNTs-CuO, MWCNTs-CuO	Water	1–5 vol%	• Turbulence elements increased HTC; HNFs outperformed water; SWCNT-CuO/water and MWCNT-CuO/water hybrids increased HTC by 8% and 4.1% at Re 10,000; 5.16% improvement in thermal efficiency with SWCNT-CuO at 1% concentration

TABLE 3 (*Continued*) Summary of Key findings on the performance of carbon-based HNFs in FPSC.

Authors	Hybrid nanoparticle	Base fluid	Concentration range	Findings
Elshazly et al. (2022)	MWCNT/Al$_2$O$_3$	Water	0.005%, 0.01%, 0.025%, and 0.05%	• Hybrid MWCNT/Al$_2$O$_3$ nanofluids increased efficiency by 26%, 29%, and 18% at flow rates of 1.5 L/m, 2.5 L/m, and 3.3 L/m, respectively
				• MWCNT nanofluid at 0.05 wt% and 3.5 L/s flow rate showed the highest efficiency, approximately 20% higher than Al$_2$O$_3$ under the same conditions
				• Exergy efficiency was enhanced by 40.5% and 34% for hybrid MWCNT/Al$_2$O$_3$ and Al$_2$O$_3$/water nanofluids, respectively, compared to distilled water

4,000 to 10,000. The HNFs outperformed pure water, with HTCs for SWCNT-CuO/water and MWCNT-CuO/water hybrids rising by 8% and 4.1% at Re 10,000, respectively. Higher concentrations of SWCNT-CuO increased both HTC and friction factor, with a 5.16% improvement in thermal efficiency observed at 1% concentration and Re 6,000 compared to non-HNFs. This research highlights the effectiveness of turbulence-inducing elements and HNFs in enhancing solar thermal systems.

The literature survey highlights the thermal performance improvements offered by HNFs in FPSCs, emphasizing various nanoparticle combinations and concentrations that enhance TC and efficiency. Hussein et al. (2020) reported a 64% increase in TC with a 0.1 wt% HNF, achieving 85% thermal efficiency. However, these enhancements are contingent on specific flow rates, temperatures, and concentrations, raising questions about their universal applicability. Additionally, Huq et al. (2023) pointed out that HNFs might not maintain their stability under dynamic flow conditions in FPSCs. A common observation is the trade-off between increased TC and higher viscosity, which can impede fluid flow, as highlighted by Verma et al. (2018) and Saleh and Sundar (2021). Therefore, careful formulation of HNFs is necessary to balance TC benefits with flow rate concerns, impacting overall collector efficiency. The choice of nanoparticle combinations also plays a significant role, with studies like those by Lee et al. (2021) suggesting that some combinations, such as MWCNT/CuO, yield greater efficiency gains.

While the results are promising, they often lack economic assessments of using HNFs in real-world applications, particularly concerning synthesis costs and maintenance issues. Huq et al. (2023) emphasized that specific nanofluid formulations must align with particular collector designs, indicating the need for tailored approaches. Moreover, integrating carbon-based HNFs with innovative turbulators has shown significant improvements in thermal efficiency, as evidenced by Negeed et al. (2023) and Ibrahim et al. (2022). However, the associated increase in pressure drop must be considered, as it could offset the energy savings from improved heat transfer. The performance variations highlighted by Ibrahim et al. (2021) and Khetib et al. (2022) further underscore the importance of optimizing turbulator design for specific operating conditions to avoid diminishing returns on efficiency. Lastly, while Nabi et al. (2022) demonstrated that turbulence-inducing elements alongside HNFs substantially improve heat transfer coefficients,
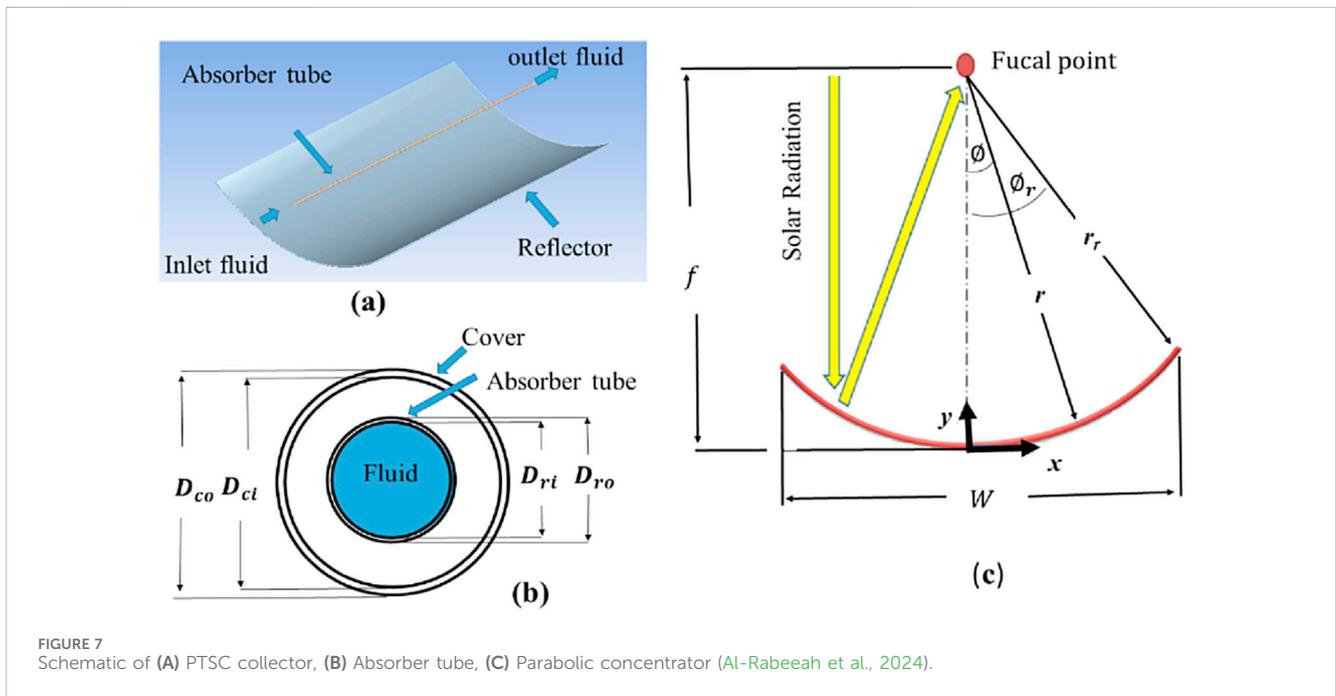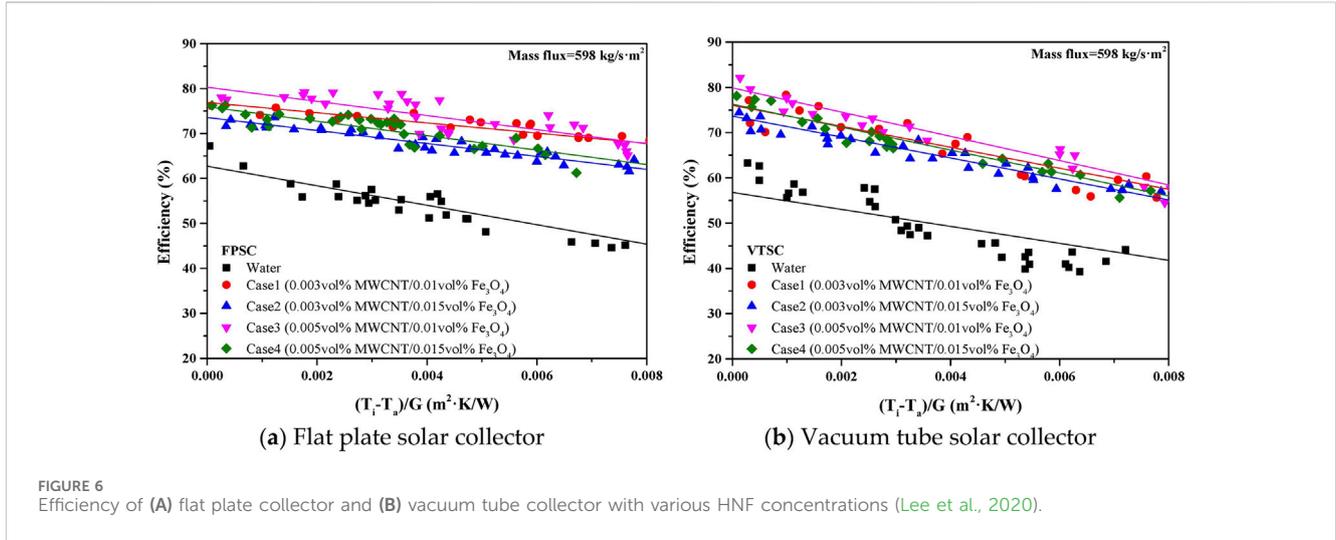
implementing these systems may require advanced control strategies and monitoring, potentially impacting costs and maintenance needs. Table 3 summarizes the key findings of the performance of FPSC using different carbon-based HNFs.

In conclusion, while the integration of carbon-based HNFs and innovative turbulators offers significant potential for enhancing solar thermal performance, careful consideration of pressure drop implications, turbulator design optimization, and practical implementation challenges is essential. Future research should focus on long-term performance assessments, cost-benefit analyses, and field testing of these advanced systems to fully understand their viability in real-world applications. By addressing these critical aspects, the solar energy sector can effectively leverage these innovations to drive further advancements in solar thermal technologies.

3.2 Parabolic concentrators and parabolic trough collectors

Parabolic concentrators and parabolic trough collectors are both solar thermal technologies that use curved mirrors to concentrate sunlight and generate heat. Figures 7A–C provides a schematic representation of a parabolic trough solar collector and its key components, including an absorber and a parabolic reflector. Recent studies have demonstrated the potential of HNFs to enhance the thermal performance and exergy efficiency of solar thermal systems, including compound parabolic concentrators (CPCs) and parabolic trough collectors (PTCs). By incorporating various nanoparticles into traditional heat transfer fluids, these systems can achieve significant improvements in heat transfer efficiency, showcasing the effectiveness of HNFs in optimizing solar energy applications.

For example, Khaledi et al. (2022) examined the thermal performance and exergy of a CPC using HNFs made of SiO$_2$ and MWCNTs in a 10% ethylene glycol and 90% distilled water mixture, with nanoparticle concentrations from 0.5 vol% to 1.5 vol% and a SiO$_2$ to MWCNT ratio of 90:10. Using Gum Arabic as a surfactant for stability, they found that TC increased with temperature and nanoparticle concentration, achieving a 12.5% improvement at 1.5 vol% and 80°C. Although viscosity decreased with temperature, it increased with nanoparticle concentration. The CPC collector's thermal efficiency improved by up to 14.27%

FIGURE 6
Efficiency of **(A)** flat plate collector and **(B)** vacuum tube collector with various HNF concentrations (Lee et al., 2020).

FIGURE 7
Schematic of **(A)** PTSC collector, **(B)** Absorber tube, **(C)** Parabolic concentrator (Al-Rabeeah et al., 2024).

over the base fluid, while exergy efficiency averaged a 45% enhancement, demonstrating the effectiveness of SiO$_2$/MWCNT HNFs in solar thermal systems.

Khan et al. (2021) investigated the thermal and thermodynamic performance of a PTC using mono and HNFs with MWCNTs and TiO$_2$ in therminol-VPI oil. The study, conducted over a temperature range of 350–600 K, revealed that HNFs in a converging-diverging tube configuration achieved a 5.27% improvement in thermal efficiency at 600 K, compared to only 0.61% with a smooth tube. The heat transfer coefficient for HNFs increased by 197.09% at 400 K, while the Nusselt number rose by 0.52% and 0.64% for smooth and converging-diverging tubes, respectively. The converging-diverging tube with HNF also showed a 2.58% increase in pumping power, while pressure drop enhancements were 0.6% for the hybrid case. The highest thermo-hydraulic performance was recorded at PEC I and II values of 1.47 and 1.33, respectively, indicating that HNFs significantly enhance the thermal, hydraulic, and thermodynamic performance of PTC systems for high-temperature solar thermal applications.

Saddouri et al. (2023) performed a thermo-mathematical numerical analysis of PTCs using HNFs composed of MWCNTs and Al$_2$O$_3$ in water. Conducted in a subtropical desert climate, their study utilized an Engineering Equation Solver (EES) for thermodynamic analysis. The results indicated that increasing nanoparticle concentration enhanced thermal efficiency, with the 1.5% MWCNT/1.5% Al$_2$O$_3$-water HNF achieving a maximum outlet fluid temperature, energy output of 5066 W, and exergy of 876 W, performing best in summer. Obalalu et al. (2023) examined heat
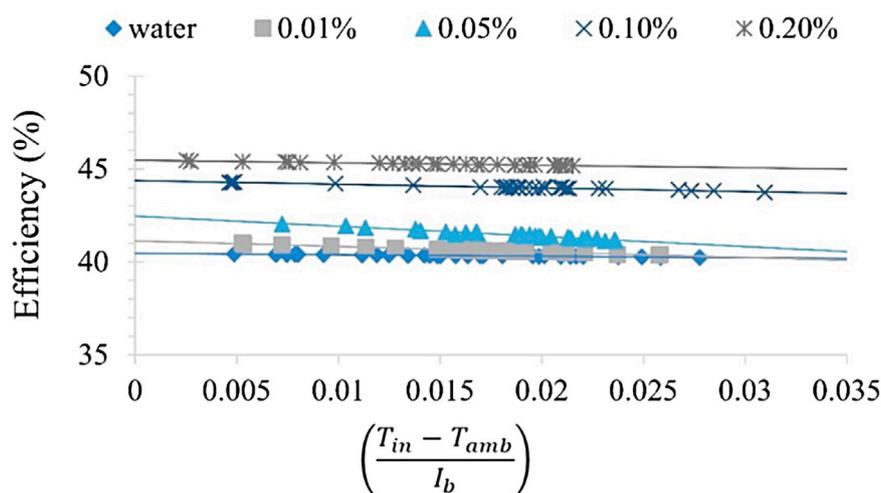
FIGURE 8
Efficiency of the solar collector using different concentrations of the HNF (Al-Rabeeah et al., 2024).

transfer enhancement in solar-powered ships using HNFs combining MWCNTs and SWCNTs in engine oil (EO) within PTCs. Although the temperature range was not specified, it likely fell between 30°C and 100°C. The study found significant improvements in TC and heat transfer efficiency, with the HNF achieving efficiency rates of approximately 1.78% and a minimum of 2.26%, showcasing HNFs' potential in optimizing solar energy solutions for maritime applications.

Al-Rabeeah et al. (2024) investigated the thermal efficiency of a PTSC using a graphene-Fe$_3$O$_4$/water HNF. Their research, which likely focused on a temperature range of 30°C–100°C, showed that TC increased with temperature and concentration. At 0.2 vol% and 60°C, the G-Fe$_3$O$_4$/water HNF's TC was 14.4% higher than that of pure water. Viscosity decreased significantly with temperature, reducing pumping power requirements and enhancing efficiency. The efficiency of a solar collector using different concentrations of a nanofluid is presented in Figure 8. The figure indicates that the PTSC achieved a maximum thermal efficiency of 45.46% with the HNF, compared to 40.41% for water, indicating the potential of graphene-based HNFs in improving solar thermal systems.

Recent research has increasingly focused on optimizing the thermal performance of parabolic solar collectors through the innovative integration of HNFs and turbulator designs. These studies highlight the significant benefits of employing twisted or conical turbulators in conjunction with HNFs, leading to enhanced heat transfer efficiency and overall system performance. For instance, Alnaqi et al. (2021) investigated the hydrothermal performance of a PTSC utilizing two twisted tape inserts and a HNF composed of MgO and MWCNTs in thermal oil (80% MgO and 20% MWCNT). The nanoparticle volume concentration varied from 0.25% to 2% by weight. For Reynolds numbers (Re) below 30,873, the liquid crystal rod-like wave (LCRW) model with a turbulator diameter of 15 mm and 2% volume fraction was recommended. In contrast, the liquid wave rod-like crystal (LWRC) model was optimal for Re exceeding 30,873. These findings highlight the potential of HNFs combined with specific turbulator designs to enhance PTSC thermal performance.

Almitani et al. (2022) examined the impact of twisted turbulators and HNFs on PSC performance. The HNFs, composed of MWCNTs and MgO in an 80:20 weight ratio suspended in water, were tested at concentrations of 1%, 2%, and 3%. Results showed that the average Nusselt number (Nuave) increased with higher Re and nanoparticle volume fractions. At a Re of 25,000% and 3% particle concentration, a pitch ratio (PR) of 1 yielded an increase of 71.25% in Nuave and 388.59% in pressure drop (Δp) compared to the PSC without a turbulator. Performance evaluation criteria exceeded 1, indicating improved PSC performance. While increasing PR enhanced thermal efficiency (ηn), exergy efficiency (ηex) decreased, with ηn and ηex improving by 45.98% and 31.67%, respectively, as Re increased from 10,000 to 25,000 for PR values of 1 and 0.25. These findings demonstrate the effectiveness of HNFs and twisted turbulators in optimizing PSCs.

Mohammed et al. (2021) studied heat transfer enhancement in PTSC receiver tubes using HNFs with conical turbulators. The HNFs included Ag-SWCNT, Ag-MWCNT, and Ag-MgO at a 50:50 mixing ratio dispersed in Syltherm oil 800. Experiments were conducted at Re from 5,000 to 100,000, and fluid inlet temperatures between 400 K and 650 K. Results indicated that conical turbulators significantly enhanced thermal performance, with the Ag-SWCNT/Syltherm oil combination achieving a 233.4% improvement over pure Syltherm oil. Performance evaluation criteria ranged from 0.9 to 1.82. Thermal and exergetic efficiencies increased by 11.5% and 18.2%, respectively, while entropy generation rate and ratio decreased by 42.7% and 33.7%, respectively. These findings underscore the effectiveness of HNFs and conical turbulators in optimizing PTSC thermal performance.

Tahmasebi et al. (2023) investigated the impact of twisted tape on the thermo-hydraulic performance and entropy generation of turbulent flow in mono and hybrid magnetic NFs within a PSC absorber tube. The study focused on water/MWCNT and water/MWCNT-iron oxide, both at a 1% nanoparticle volume fraction. Results showed that twisted tape significantly enhanced thermo-hydraulic performance, yielding a performance coefficient above 1.

The use of magnetic NFs improved thermal performance due to their magnetic properties and better flow characteristics from the twisted tape. Entropy generation decreased with increasing Reynolds number and pitch ratio, indicating that optimizing these factors can minimize energy losses and enhance efficiency. Overall, the findings highlight the effectiveness of twisted tape in improving heat transfer and energy efficiency in solar collectors, particularly with hybrid magnetic NFs.

Hosseini Esfahani et al. (2023) studied the effects of twisted tape (TT) and compound twisted tape (CTT) turbulators on the performance of a PTC, assessing energy, economic, and environmental efficiencies. The HNF comprised CuO and SWCNT dispersed in water, with nanoparticle concentrations varying from 2% to 6%. The incorporation of turbulators significantly enhanced the Nusselt number and friction coefficient, improving the thermal performance of the PTC. The CuO-SWCNT/water HNF outperformed water-based fluids, with heat transfer rates improving by 20%–60%. Economic analysis revealed that increasing flow velocity and nanoparticle volume fraction reduced the Levelized Cost of Energy (LCOE), suggesting potential cost-effectiveness for solar thermal systems. Environmentally, the HNF produced fewer pollutants than conventional fluids, enhancing sustainability. The thermal performance of the PTC with CTT and wired coil was 3.58% higher than that with standard TT at a Reynolds number of 18,000 and a 2% nanoparticle concentration. However, exergy efficiency decreased by 31.7% and 32.2% with increased flow velocity for the PTC with TT and CTT, respectively. Overall, the research highlights the effectiveness of turbulators and NFs in enhancing the thermal, economic, and environmental performance of PTCs, suggesting modifications for more efficient and sustainable solar thermal energy systems.

Integrating HNFs into parabolic solar collectors offers significant potential for enhancing thermal performance, yet optimizing these systems is complex. Khaledi et al. (2022) found that while HNFs can improve TC and exergy efficiency, higher nanoparticle concentrations may lead to diminishing returns due to increased viscosity. Khan et al. (2021) echoed this, highlighting challenges in balancing thermal efficiency with pumping power and pressure drop. In maritime applications, Obalalu et al. (2023) showed that HNFs enhance heat transfer in solar-powered vessels, although scalability remains a concern. Al-Rabeeah et al. (2024) noted that viscosity reductions at elevated temperatures do not uniformly improve performance across different collector designs.

Furthermore, Alnaqi et al. (2021) and Almitani et al. (2022) emphasized the importance of flow modifications, like twisted or conical turbulators, in optimizing thermal performance. These modifications, alongside HNFs, led to notable improvements in Nusselt numbers and energy capture. However, questions about cost-effectiveness and manufacturing feasibility persist. Studies by Mohammed et al. (2021) and Tahmasebi et al. (2023) revealed that HNFs enhance thermal efficiency and reduce entropy generation, which is essential for sustainability. Table 4 summarizes the key findings of the performance of PSC and PTSC using different carbon-based HNFs.

In summary, while research indicates substantial advancements in parabolic solar collectors using HNFs, a nuanced approach is needed to balance nanoparticle selection, concentration, and system

design. Future studies should focus on the long-term stability of these NFs, their environmental impact, and practical guidelines for diverse solar thermal applications to translate laboratory success into real-world solutions.

3.3 Direct absorption solar collectors

A Direct Absorption Solar Collector (DASC) is a type of solar thermal collector where sunlight is absorbed directly by a working fluid rather than being absorbed by a solid surface and then transferred to the fluid. This direct absorption method offers several advantages, including higher efficiency, reduced heat loss, and simpler design. Figure 9 provides a schematic representation of a DASC.

HNFs are emerging as promising candidates for enhancing the efficiency of direct absorption solar collectors (DASCs) through improved thermal properties and stability. Recent studies have explored various combinations of materials, including nitrogen-doped reduced GO (rGO), MWCNTs, SiC, and metal-based nanoparticles. These investigations demonstrate significant enhancements in TC, solar-thermal conversion efficiency, and overall stability, paving the way for advanced solar thermal applications. Shende and Sundara (2015) investigated nitrogen-doped hybrid structures of rGO and MWCNTs as nanofluids in DASCs. They prepared HNFs by dispersing nitrogen-doped rGO-MWCNTs in deionized water and ethylene glycol, using surfactants like polyethylene glycol (PEG) and sodium lauryl sulfate (SLS) for stability. The results indicated a 17.7% increase in TC at a 0.02% volume fraction in water and a 15.1% increase at 0.03% in ethylene glycol, highlighting the potential of these HNFs to enhance solar thermal system performance. The nanofluids also exhibited excellent stability with minimal agglomeration due to the percolation network formed by MWCNTs within rGO layers.

Li et al. (2020) studied the stability, optical properties, and solar-thermal conversion performance of SiC and MWCNTs HNFs for DASCs. The study utilized SiC-MWCNTs in, EG with mass fractions from 0.01 wt% to 1 wt%. The HNFs demonstrated excellent stability, confirmed by static experiments and Zeta potential measurements. They exhibited strong solar absorption (99.9% at 0.5 wt% over 1 cm) and improved solar-thermal conversion efficiency, reaching 97.3% with a 1 wt% nanofluid, a 48.6% enhancement over pure, EG. Overall, SiC-MWCNTs HNFs show significant promise for improving DASC performance through enhanced stability and solar-thermal efficiency.

Mehrali et al. (2018) investigated hybrid plasmonic nanofluids comprising rGO decorated with silver nanoparticles for volumetric solar absorbers. They examined how variations in the mass fraction of graphene nanosheets and silver content influenced the thermal and optical properties of these HNFs. Results indicated that the nanofluids could be effectively used in DASCs, achieving a collector efficiency of 77% at a concentration of just 40 parts per million (ppm). This efficiency is attributed to the enhanced light absorption capabilities of graphene at specific excitation wavelengths, highlighting the potential of rGO decorated with silver nanoparticles to improve volumetric solar absorber performance.

Zeng and Xuan (2018) studied the solar thermal conversion and thermal conduction properties of MWCNT and silica/silver

TABLE 4 Summary of Key findings on the performance of carbon-based HNFs in PTC.

Authors	Hybrid nanoparticle	Base fluid	Concentration range	Findings
Khaledi et al. (2022)	SiO$_2$/MWCNTs (90:10)	10% ethylene glycol, 90% distilled water	0.5–1.5 vol%	• TC increased with temperature and nanoparticle concentration (12.5% improvement at 1.5 vol% and 80°C); thermal efficiency improved by up to 14.27%; exergy efficiency improved by 45%
Khan et al. (2021)	MWCNTs, TiO$_2$	Therminol-VPI oil	1.5% HNF, 3% Mono NF	• HNFs in converging-diverging tubes improved thermal efficiency by 5.27% at 600 K; the heat transfer coefficient increased by 197.09% at 400 K
Saddouri et al. (2023)	MWCNTs, Al$_2$O$_3$	Water	1.5%	• Increased nanoparticle concentration enhanced thermal efficiency; 1.5% MWCNT/1.5% Al$_2$O$_3$-water HNF achieved maximum outlet fluid temperature and energy output
Al-Rabeeah et al. (2024)	Graphene-Fe$_3$O$_4$	Water	0.01–0.2 vol%	• TC increased with temperature and concentration (14.4% higher than water at 0.2 vol% and 60°C); viscosity decreased with temperature
				• The highest efficiency (45.46%) was achieved with a 0.2% volume concentration of the HNF. Efficiency decreased with lower concentrations (0.1%, 0.05%, 0.01%)
Alnaqi et al. (2021)	MgO/MWCNTs (80:20)	Thermal oil	0.25–2 wt%	• Different twisted tape inserts and HNFs enhanced PTSC thermal performance; optimal configuration depended on the Reynolds number
Almitani et al. (2022)	MWCNTs/MgO (80:20)	Water	1%, 2%, 3%	• Nuave increased with Re and nanoparticle volume fractions; twisted turbulators with specific PR improved Nuave and thermal efficiency
Mohammed et al. (2021)	Ag-SWCNT, Ag-MWCNT, Ag-MgO (50:50)	Syltherm oil 800	1%–3%	• Conical turbulators and HNFs significantly enhanced thermal performance; Ag-SWCNT/Syltherm oil showed a 233.4% improvement
Tahmasebi et al. (2023)	Water/MWCNT-iron oxide	Water	1%	• Twisted tape enhanced thermo-hydraulic performance; magnetic NFs improved thermal performance; entropy generation decreased with increasing Reynolds number and pitch ratio
Hosseini Esfahani et al. (2023)	CuO, SWCNT	Water	2%–6%	• Turbulators and HNFs enhanced Nusselt number and friction coefficient; CuO-SWCNT/water HNF improved heat transfer rates by 20%–60%; economic and environmental benefits were observed

FIGURE 9
DASC schematic (Karami et al., 2014).
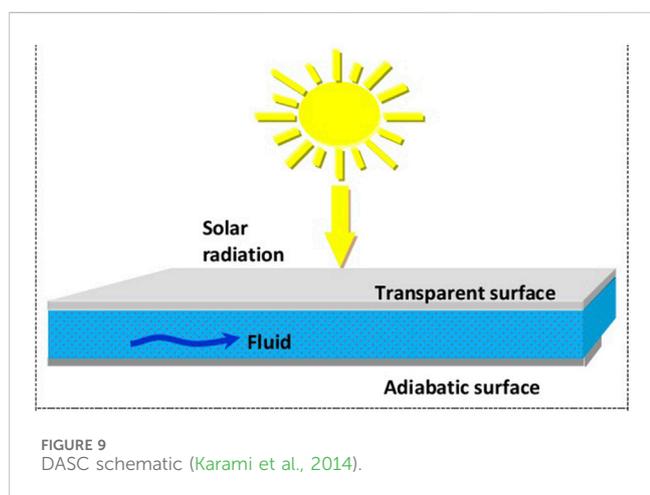
(SiO$_2$/Ag) binary nanofluids. By varying the volume fraction of nanomaterials from 0.001% to 0.1% and adjusting the MWCNT to SiO$_2$/Ag ratio between 4:1 and 1:4, they optimized the absorptance of

the nanofluids. A 0.1% MWCNT volume fraction enhanced TC by about 7%, and the binary nanofluid achieved photo-thermal conversion efficiencies of 97.6% at 35°C and 42.7% at 70°C, demonstrating its potential for solar thermal energy applications.

Qu et al. (2019) investigated the photo-thermal conversion properties of hybrid CuO-MWCNT/H2O nanofluids for direct solar thermal energy harvesting. They prepared water-based HNFs using varying concentration mixing ratios (CMRs) of CuO and MWCNTs from 0.01 wt%/0.0015 wt% to 0.25 wt%/0.0015 wt%. Findings revealed that CuO-MWCNT nanofluids exhibited significantly enhanced solar spectral absorption compared to individual CuO or MWCNT nanofluids, achieving nearly 100% solar-weighted absorption at a 1 cm optical penetration distance. The optimal CMR of 0.15 wt%/0.005 wt% achieved a maximum terminal temperature rise of 14.1°C compared to deionized water after 45 min of light irradiation, showcasing the potential of CuO-MWCNT HNFs to enhance solar thermal energy conversion efficiency.

Campos et al. (2019) explored the impact of particle shape and GO on the performance of DASCs using metal-based nanofluids. Their study included spherical gold, silver, and copper
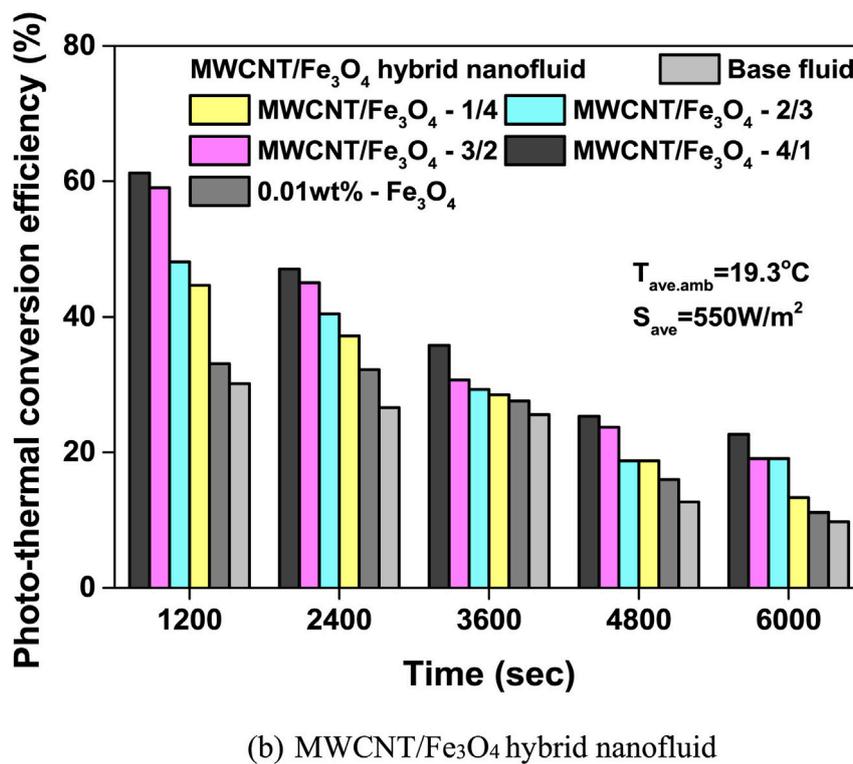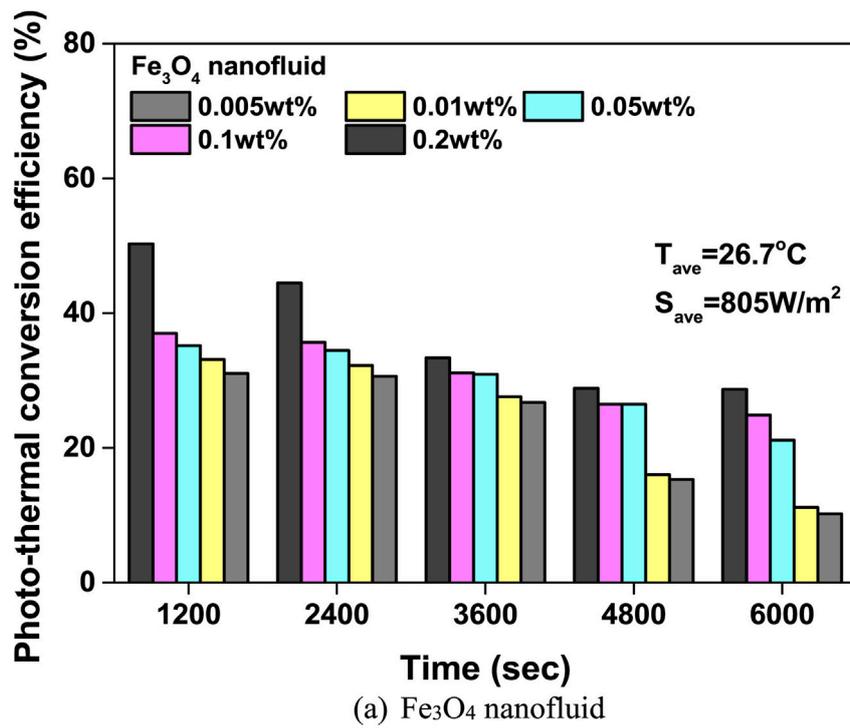
FIGURE 10
Efficiency against time for a DASC with **(A)** mono-Fe_3O_4 nanofluids and **(B)** different MWCNT/Fe_3O_4 HNFs (Tong et al., 2020).

nanoparticles, nonspherical silver nanoparticles, layered GO, and GO/silver hybrids. Results showed that all nanofluids had thermal conductivities about 4% higher than pure water, deviating from Maxwell model predictions. Under 1 Sun simulated solar radiation, spherical metal nanofluids raised temperatures by up to 5 K,

achieving 35% higher efficiencies than pure water after 3,000 s. Nonspherical silver nanoparticles and GO/silver hybrids demonstrated approximately 20% greater efficiencies than conventional spherical silver nanofluids. In natural solar conditions with a parabolic dish mirror (60 concentration ratio),

temperature increases reach up to 50 K, doubling the efficiency of pure water. Additionally, nonspherical silver nanofluids and GO/silver hybrids generated steam faster than spherical silver nanofluids, indicating superior performance in solar thermal applications.

In their investigation, Tong et al. (2020) investigated the photo-thermal energy conversion performance of Fe_3O_4 and multi-walled carbon nanotube (MWCNT)/Fe_3O_4 HNFs. The addition of MWCNTs significantly enhanced energy conversion, with both nanofluids showing increased temperatures over time. The MWCNT/Fe_3O_4 HNF achieved a faster temperature rise due to its superior thermal properties, reaching a maximum increase of 5.5°C at a 4:1 mixing ratio, while the Fe_3O_4 nanofluid increased by 6.4 °C at 0.2 wt%. Although efficiencies decreased over time due to heat loss, the MWCNT/Fe_3O_4 HNF maintained higher efficiency, dropping from 61% to 22%, compared to 33%–11% for the Fe_3O_4 nanofluid as presented in Figures 10A, B. Temperature distribution analysis showed that the upper section of the HNFs absorbed most solar energy, particularly for the MWCNT/Fe_3O_4 hybrid. The total stored energy in the HNFs increased with MWCNT inclusion, peaking at 2,400 kJ/kg at the optimal 4:1 mixing ratio, a 26.6% enhancement over the base fluid, highlighting the potential of MWCNT/Fe_3O_4 HNFs for improved thermal efficiency.

Mashhadian et al. (2021) studied the influence of HNFs composed of Al_2O_3 and MWCNTs in water on the performance of direct absorption parabolic trough collectors (DAPTCs). With nanoparticle concentrations from 0.01 vol% to 0.04 vol%, HNFs exhibited superior optical properties compared to mono nanofluids and water. At 0.04 vol%, HNFs increased the maximum temperature difference of the collector by 240.7% over water, 57.2% over 0.04% alumina, and 8.2% over 0.04% MWCNTs, while improving thermal efficiency by 197.1%, 69.2%, and 6.1%, respectively. The pressure drop associated with HNFs was negligible, indicating minimal impact on system operation. Environmentally, HNFs reduced CO_2 emissions and water consumption by 450.33 kg and 2016.6 m³ per collector, respectively, underscoring their potential to enhance thermal performance and sustainability in solar energy systems.

The studies presented demonstrate significant advancements in the application of HNFs for DASCs, highlighting their enhanced thermal properties and performance capabilities. Shende and Sundara (2015) showed notable improvements in TC using nitrogen-doped rGO-MWNTs, effectively mitigating agglomeration. However, the lack of long-term performance data limits practical applications in solar thermal systems. Li et al. (2020) confirmed the promise of HNFs, showcasing robust stability and impressive solar-thermal conversion efficiency with their SiC-MWCNTs. While their findings emphasize practical applications, they are restricted to specific concentration ranges, necessitating broader investigations for optimal conditions. Mehrali et al. (2018) integrated silver nanoparticles with reduced GOs, achieving high collector efficiencies even under low illumination. Still, the scalability of these HNFs for commercial applications remains unexamined, revealing a gap in transitioning from laboratory successes to field applications.

Zeng and Xuan (2018) highlighted the tunability of HNF performance through material ratio adjustments. However, their limited volume fraction range restricts broader applicability, indicating a need for further exploration of diverse compositions to assess their impact on thermal properties and efficiency. Qu et al.

(2019) provided insights into the synergy between CuO and MWCNTs but noted that performance heavily depends on specific concentration mixing ratios, emphasizing the complexity of formulating effective HNFs. Campos et al. (2019) revealed the significant impact of particle shape and composition on TC and photo-thermal conversion efficiency, suggesting that nonspherical nanoparticles may enhance performance. However, these findings raise questions about reproducibility across different experimental setups and real-world applications. Mashhadian et al. (2021) examined the environmental sustainability of HNFs, demonstrating substantial reductions in CO_2 emissions and water consumption, yet the absence of comprehensive lifecycle analysis limits understanding of their ecological impacts. Table 5 summarizes the key findings of the performance of DASC using different carbon-based HNFs.

In summary, while these studies underscore the potential of HNFs in advancing DASCs, they also highlight critical gaps in long-term stability, scalability, and ecological implications. Further research in these areas is essential for leveraging HNFs in practical and sustainable solar energy applications.

4 Discussion

The use of carbon-based HNFs in solar thermal applications presents advancements in heat transfer efficiency, but several challenges persist. Integrating materials like graphene and carbon nanotubes (CNTs), these nanofluids significantly enhance TC in solar collectors, which is crucial for boosting overall efficiency. However, while these enhancements are promising, limitations must be addressed for practical application.

A primary advantage of carbon-based HNFs is their enhanced TC, which is essential for improving the efficiency of solar collectors. Studies, including Borode et al., 2023a, report substantial increases in TC when combining graphene and metal nanoparticles, often surpassing some single-component nanofluids. For example, Borode et al. (2021) observed an enhancement in TC with a graphene-alumina HNF, highlighting the synergistic effect of carbon materials and metallic nanoparticles. These findings align with Jin et al. (2024) and Shahsavar et al. (2015), who also found significant improvements with graphene and CNT hybrids. The inherent TC of graphene, due to its two-dimensional structure and high electron mobility, is critical in this enhancement. Similarly, CNTs create efficient thermal pathways when integrated into the base fluid.

Several studies demonstrate the efficacy of carbon-based HNFs in solar thermal systems, particularly in FPSC and PTCs. Hussein et al. (2020) investigated a water-based HNF containing functionalized MWCNTs and hBN in a flat-plate solar collector, achieving a 64% increase in TC at 60°C and a 20% overall improvement in thermal efficiency, reaching up to 85%. Verma et al. (2018) examined flat-plate collectors using CuO and MgO HNFs combined with MWCNTs, reporting exergy and energy efficiencies of 71.54% and 70.55%, respectively, with MgO hybrid outperforming CuO, emphasizing the importance of nanoparticle selection.

PTCs, requiring higher operating temperatures for industrial applications, have also benefited from carbon-based HNFs. Lee et al. (2020) studied MWCNT and Fe_3O_4 binary nanofluids in flat-plate and vacuum tube collectors, revealing a 17.6% efficiency increase in

TABLE 5 Summary of Key findings on the performance of carbon-based HNFs in DASC.

Authors	Hybrid nanoparticle	Base fluid	Concentration range	Key findings
Shende and Sundara (2015)	Nitrogen-doped rGO-MWCNTs	Deionized water, ethylene glycol	0.02 vol% (water), 0.03 vol% (EG)	• 17.7% increase in TC in water, 15.1% increase in ethylene glycol; excellent stability • The nanofluid exhibits strong optical absorption, which increases with higher concentrations of nanoparticles
Li et al. (2020)	SiC-MWCNTs	Ethylene glycol (EG)	0.01 wt% to 1 wt%	• Excellent stability; strong solar absorption (99.9% at 0.5 wt%) • Improved solar-thermal conversion efficiency (97.3% at 1 wt%)
Mehrali et al. (2018)	rGO decorated Ag nanoparticles	Deionized Water	40 ppm	• Collector efficiency of 77% at 40 ppm due to enhanced light absorption
Zeng and Xuan (2018)	MWCNT and silica/silver (SiO$_2$/Ag)	Deionized Water	0.001%–0.1%	• 0.1% MWCNT enhanced TC by 7%; binary nanofluid achieved photo-thermal conversion efficiencies of 97.6% at 35°C and 42.7% at 70°C
Qu et al. (2019)	CuO-MWCNT	Water	0.01 wt%/0.0015 wt% to 0.25 wt%/0.0015 wt%	• Enhanced solar spectral absorption; optimal CMR of 0.15 wt%/0.005 wt% achieved a maximum temperature rise of 14.1°C
Tong et al. (2020)	MWCNT/Fe$_3$O$_4$	Ethylene glycol/water (2:8)	0.005–0.2 wt%	• MWCNTs enhanced energy conversion and thermal properties of the Fe$_3$O$_4$ nanofluid • MWCNT/Fe$_3$O$_4$ HNF achieved faster temperature rise (5.5°C at 4:1 mixing ratio); higher efficiency maintained over time • At 0.2 wt% MWCNT/Fe$_3$O$_4$ hybrid nanofluid, the photo-thermal energy conversion efficiency was 32.8% and 45.1% with the absence and presence of an external magnetic field • The increase in magnetic force significantly improved the TC of the nanofluids
Mashhadian et al. (2021)	Al$_2$O$_3$ and MWCNTs	Water	0.01 vol% to 0.04 vol%	• HNFs showed superior optical properties • at 0.04 vol%, HNFs increased the maximum temperature difference by 240.7% and thermal efficiency by 197.1% compared to water • negligible pressure drop
Bao et al. (2023)	MWCNT/SiC	Deionized water	0–10ppm MWCNT/0–80ppm SiC	• HNF absorbs a wider spectrum of sunlight and performs better than single-component nanofluids • HNF with 5 ppm MWCNTs and 40 ppm SiC achieves 64.7% (highest) photothermal conversion efficiency
Zheng et al. (2022)	MWCNT/TiN	Deionized water	0–30ppm MWCNT/0–20ppm TiN	• Adding TiN to MWCNT nanofluids increased the absorption of sunlight • The hybrid nanofluid with 10 ppm of both MWCNT and TiN showed the highest efficiency, outperforming the base fluid and single-component nanofluids • The solar-weighted absorption fraction of hybrid MWCNT-TIN nanofluids at a depth of 4 cm increased up to 96.5%, 98.6%, 99.6%, and 99.9% from 89.8% for the mass fraction of TiN at 5, 10, 15, and 20 ppm, respectively • The highest efficiency of the hybrid MWCNT-TIN nanofluids was achieved at the MWCNT/TIN mass fraction of 10 ppm/10 ppm, which increased by 6.9%, 6.0%, and 3.8% at 2000, 4,000, and 6,000 s, compared to the baseline of the MWCNT nanofluid at 10 ppm
Shin et al. (2020)	MWCNT/Fe$_3$O$_4$	Ethylene glycol/water (2:8)	0.005–0.2 wt%	• An external magnetic field enhanced the photo-thermal energy conversion efficiency

TABLE 5 *(Continued)* Summary of Key findings on the performance of carbon-based HNFs in DASC.

Authors	Hybrid nanoparticle	Base fluid	Concentration range	Key findings
				• At 0.2 wt% MWCNT/Fe_3O_4 hybrid nanofluid, the photo-thermal energy conversion efficiency was 32.8% and 45.1% with the absence and presence of an external magnetic field
				• Adding MWCNT nanoparticles increased the thermal properties of the Fe_3O_4 nanofluid
				• The increase in magnetic force significantly improved the TC of the nanofluids
Struchalin et al. (2022)	Fe_3O_4/MWCNT	Water-10% wt. Ethanol	0.0053% of Fe_3O_4 and 0.0045% of MWCNT	• The thermal efficiency of the DASC with hybrid nanofluid was in the range of 52.3%–69.4%, slightly higher than the collector with surface absorption
				• The MWCNT nanofluid of the same concentration had 8.3%–31.5% higher efficiency than the hybrid nanofluid
				• The HNF had a lower extinction coefficient and absorbed less light than the MWCNT nanofluid
				• The optimum flow rate for maximum efficiency was 6 L/min. The turbulent mixing of the nanofluid reduced the surface temperature at high flow rates

flat-plate collectors and a 24.9% improvement in vacuum tube collectors compared to water alone. This significant increase in efficiency underscores the potential of HNFs in high-temperature applications where conventional fluids often fall short.

Despite these results, critical limitations exist. A notable concern is the increase in viscosity observed with higher nanoparticle concentrations. Kishore et al. (2020) found that a 9.95% improvement in TC was accompanied by a 13.83% increase in viscosity, highlighting the delicate trade-off between thermal and rheological properties. Increased viscosity can impede fluid flow, leading to higher pumping power requirements, which may negate energy savings from improved heat transfer. Verma et al. (2018) reported that higher nanoparticle concentrations lead to increased viscosity, negatively affecting fluid flow and raising pumping power needs. This issue is particularly pronounced in large-scale systems where fluid must circulate efficiently. Syam Sundar et al., 2017 reported substantial rises in viscosity with GO and Co_3O_4 HNFs, which hindered overall system performance despite significant TC gains. Jin et al. (2024) emphasized the need to manage the trade-off between TC and viscosity to avoid undermining system efficiency. Future research should explore surface modifications or stabilizers to reduce viscosity while maintaining improved thermal properties.

Another critical issue is the long-term stability of HNFs under operational conditions. Nanoparticle agglomeration, sedimentation, and viscosity changes can significantly impair solar thermal efficiency. Although short-term TC improvements have been shown, limited data exists on nanofluid performance in dynamic environments over extended periods. Jin et al. (2024) reported that HNFs maintained improved TC over time but did not fully address agglomeration and sedimentation risks. Studies like Borode et al. (2021) focused on short-term thermal performance without assessing the sustainability of improvements in dynamic conditions. This gap is significant as instability can lead to degradation and increased maintenance needs in dynamic solar systems. Fluctuating temperatures, high shear forces, and exposure to solar radiation may further accelerate degradation or

alter fluid properties. Future research should prioritize evaluating long-term performance under varying environmental and operational conditions, focusing on maintaining nanoparticle dispersion and preventing agglomeration. Strategies such as surface modifications, stabilizing agents, and real-time fluid property monitoring could help mitigate these challenges.

SHC also requires attention, as solar thermal systems depend on working fluids to store thermal energy, especially during intermittent sunlight. While HNFs improve heat transfer, they often reduce the specific heat of the fluid. Yarmand et al., 2016a noted a 6.26% decrease in specific heat in GNP-platinum HNFs, limiting applicability in systems needing substantial energy storage. This trade-off highlights the need for novel nanoparticle combinations that maintain or enhance heat storage capacity. Future research should explore integrating materials with higher specific heat or incorporating non-metallic additives to counterbalance reductions.

Despite their promise, the economic feasibility of large-scale adoption of carbon-based HNFs poses challenges. Comprehensive studies on scaling up for industrial use are lacking, with most research focusing on laboratory results without addressing costs. While metals like silver enhance thermal performance, their high cost limits practicality. Mehrali et al. (2018) noted substantial TC improvements with graphene-silver hybrids but emphasized silver's cost constraints. Future studies should explore cost-effective alternatives, such as copper or nickel, which offer similar thermal enhancements at lower prices. Optimizing nanoparticle concentrations could maximize thermal performance while minimizing costs. Addressing economic barriers is crucial for transitioning HNFs from research to commercially viable solutions in solar thermal systems.

Additionally, the environmental and health safety impacts of increased nanoparticle concentration in HNFs are not fully understood. Nanoparticles pose risks to human health and the environment if mismanaged, especially in systems prone to leakage or improper disposal. While current research primarily

focuses on thermal performance, future studies should evaluate environmental impacts and safety protocols necessary for widespread industrial application.

5 Conclusion

This review highlights the potential of carbon-based HNFs in enhancing solar thermal energy systems. Carbon-based nanomaterials, particularly graphene and multi-walled carbon nanotubes, offer exceptional thermal properties that can improve the efficiency of solar thermal collectors. Combining these nanoparticles with metallic counterparts in HNFs enhances TC, heat transfer rates, and stability compared to single-component nanofluids. The studies reviewed demonstrate that carbon-based HNFs can significantly enhance the performance of various solar thermal systems, contributing to a more efficient and sustainable energy future.

However, challenges remain in utilizing carbon-based HNFs for solar thermal applications. A key issue is balancing the increased TC with the accompanying rise in viscosity, which can impede fluid flow and require higher pumping power, potentially offsetting energy efficiency gains. Long-term stability under operational conditions is also a concern, as particle agglomeration and sedimentation can reduce effectiveness over time. Moreover, the reduction in SHC observed with HNFs may limit their applicability in systems requiring substantial energy storage.

Future research should focus on reducing HNF viscosity while maintaining or enhancing TC, improving long-term stability in high-temperature systems, and designing HNFs that retain or improve SHC. Evaluating the economic feasibility and environmental impact of using HNFs at scale is essential, as is exploring their applicability in solar thermal technologies beyond flat-plate and parabolic trough collectors. In conclusion, addressing these challenges will help maximize the potential of carbon-based HNFs in solar energy systems, offering sustainable solutions for both residential and industrial applications.

Author contributions

AB: Conceptualization, Formal Analysis, Writing–original draft. TT: Formal Analysis, Writing–review and editing. PO: Resources, Supervision, Writing–review and editing.

Conflict of interest

The authors declare that the research was conducted in the absence of any commercial or financial relationships that could be construed as a potential conflict of interest.

Generative AI statement

The author(s) declare that Generative AI was used in the creation of this manuscript. The authors declare that during the preparation of this work, generative AI and AI-assisted technologies were used to help check for grammatical errors and improve the manuscript's readability. The specific tools used were ChatGPT-4 and Grammarly. After using these tools, the authors reviewed and edited the content as needed and take full responsibility for the content of the publication.

Publisher's note

All claims expressed in this article are solely those of the authors and do not necessarily represent those of their affiliated organizations, or those of the publisher, the editors and the reviewers. Any product that may be evaluated in this article, or claim that may be made by its manufacturer, is not guaranteed or endorsed by the publisher.

References

AbdEl-Rady Abu-Zeid, M., Elhenawy, Y., Bassyouni, M., Majozi, T., Toderas, M., Al-Qabandi, O. A., et al. (2024). Performance enhancement of flat-plate and parabolic trough solar collector using nanofluid for water heating application. *Results Eng.* 21, 101673. doi:10.1016/J.RINENG.2023.101673

Ahammed, N., Asirvatham, L. G., Titus, J., Bose, J. R., and Wongwises, S. (2016). Measurement of thermal conductivity of graphene–water nanofluid at below and above ambient temperatures. *Int. Commun. Heat Mass Transf.* 70, 66–74. doi:10.1016/j.icheatmasstransfer.2015.11.002

Ahmed, M., Meteab, M. M., Salih, Q. O., Mohammed, H. A., and Alawi, O. A. (2022). Experimental investigation on the thermophysical and rheological behavior of aqueous dual hybrid nanofluid in flat plate solar collectors. *Energies* 15, 8541. doi:10.3390/EN15228541

Ajbar, W., Hernández, J. A., Parrales, A., and Torres, L. (2023). Thermal efficiency improvement of parabolic trough solar collector using different kinds of hybrid nanofluids. *Case Stud. Therm. Eng.* 42, 102759. doi:10.1016/J.CSITE.2023.102759

Akhgar, A., and Toghraie, D. (2018). An experimental study on the stability and thermal conductivity of water-ethylene glycol/TiO2-MWCNTs hybrid nanofluid: developing a new correlation. *Powder Technol.* 338, 806–818. doi:10.1016/J.POWTEC.2018.07.086

Alfellag, M. A., Kamar, H. M., Abidin, U., Kazi, S. N., Sidik, N. A. C., Muhsan, A. S., et al. (2024). Optimizing mixing ratio of multi-walled carbon nanotubes and titanium dioxide: a green approach to high-performance hybrid nanofluids for heat transfer. *Powder Technol.* 436, 119509. doi:10.1016/J.POWTEC.2024.119509

Almitani, K. H., Alzaed, A., Alahmadi, A., Sharifpur, M., and Momin, M. (2022). The influence of the geometric shape of the symmetrical twisted turbulator on the performance of parabolic solar collector having hybrid nanofluid: numerical approach using two-phase model. *Sustain. Energy Technol. Assessments* 51, 101882. doi:10.1016/J.SETA.2021.101882

Alnaqi, A. A., Alsarraf, J., and Al-Rashed, A. A. A. A. (2021). Hydrothermal effects of using two twisted tape inserts in a parabolic trough solar collector filled with MgO-

MWCNT/thermal oil hybrid nanofluid. *Sustain. Energy Technol. Assessments* 47, 101331. doi:10.1016/J.SETA.2021.101331

Al-Rabeeah, A. Y., Seres, I., and Farkas, I. (2022). Recent improvements of the optical and thermal performance of the parabolic trough solar collector systems. Facta universitatis. *Ser. Mech. Eng.* 20, 073–094. doi:10.22190/FUME201106030A

Al-Rabeeah, A. Y., Seres, I., and Farkas, I. (2024). Experimental and numerical investigation of parabolic trough solar collector thermal efficiency enhanced by graphene–Fe3O4/water hybrid nanofluid. *Results Eng.* 21, 101887. doi:10.1016/J.RINENG.2024.101887

Alsangur, R., Doganay, S., Ates Turgut, A., Cetin, L., and Rebay, M. (2024). Magnetic field dependent thermal conductivity investigation of water based Fe3O4/CNT and Fe3O4/graphene magnetic hybrid nanofluids using a Helmholtz coil system setup. *Diam. Relat. Mater* 141, 110716. doi:10.1016/J.DIAMOND.2023.110716

Alam, T., Balam, N. B., Kulkarni, K. S., Siddiqui, M. I. H., Kapoor, N. R., Meena, C. S., et al. (2021). Performance augmentation of the flat plate solar thermal collector: A review. *Energies* 14 (19), 6203. doi:10.3390/EN14196203

Asaad Yasseen, A. R., Istvan, S., and Istvan, F. (2022). Selective absorber coatings and technological advancements in performance enhancement for parabolic trough solar collector. *J. Therm. Sci.* 31 (6 31), 1990–2008. doi:10.1007/S11630-022-1634-5

Askari, S., Koolivand, H., Pourkhalil, M., Lotfi, R., and Rashidi, A. (2017). Investigation of Fe 3 O 4/Graphene nanohybrid heat transfer properties: experimental approach. *Int. Commun. Heat Mass Transf.* 87, 30–39. doi:10.1016/J.ICHEATMASSTRANSFER.2017.06.012

Atta, N., Galal, A., and Nanoscale, E.E.-A.-B. (2015). Graphene—a platform for sensor and biosensor applications. *Biosensors-Micro Nanoscale Appl.* doi:10.5772/60676

Babar, H., Sajid, M., and Ali, H. (2019). Viscosity of hybrid nanofluids: a critical review. *Therm. Sci.* 23, 1713–1754. doi:10.2298/TSCI181128015B

Bakhtiari, R., Kamkari, B., Afrand, M., and Abdollahi, A. (2021). Preparation of stable TiO2-Graphene/Water hybrid nanofluids and development of a new correlation for thermal conductivity. *Powder Technol.* 385, 466–477. doi:10.1016/j.powtec.2021.03.010

Balaga, R., Ramji, K., Subrahmanyam, T., and Babu, K. R. (2019). Effect of temperature, total weight concentration and ratio of Fe2O3 and f-MWCNTs on thermal conductivity of water based hybrid nanofluids. *Mater Today Proc.* 18, 4992–4999. doi:10.1016/J.MATPR.2019.07.492

Balaji, T., Rajendiran, S., Selvam, C., and Lal, D. M. (2021). Enhanced heat transfer characteristics of water based hybrid nanofluids with graphene nanoplatelets and multi walled carbon nanotubes. *Powder Technol.* 394, 1141–1157. doi:10.1016/j.powtec.2021.09.014

Bao, Y., Huang, A., Zheng, X., and Qin, G. (2023). Enhanced photothermal conversion performance of MWCNT/SiC hybrid aqueous nanofluids in direct absorption solar collectors. *J. Mol. Liq.* 387, 122577. doi:10.1016/J.MOLLIQ.2023.122577

Bellos, E., Korres, D., Tzivanidis, C., and Antonopoulos, K. A. (2016). Design, simulation and optimization of a compound parabolic collector. *Sustain. Energy Technol. Assessments* 16, 53–63. doi:10.1016/J.SETA.2016.04.005

Bellos, E., and Tzivanidis, C. (2017). Parametric analysis and optimization of an Organic Rankine Cycle with nanofluid based solar parabolic trough collectors. *Renew. Energy* 114, 1376–1393. doi:10.1016/J.RENENE.2017.06.055

Borode, A., Tshephe, T., Olubambi, P., Sharifpur, M., and Meyer, J. (2023a). Stability and thermophysical properties of GNP-Fe2O3 hybrid nanofluid: effect of volume fraction and temperature. *Nanomaterials* 13, 1238. doi:10.3390/nano13071238

Borode, A., Tshephe, T., Olubambi, P., Sharifpur, M., and Meyer, J. (2023b). Experimental study and ANFIS modelling of the thermophysical properties and efficacy of GNP-Al2O3 hybrid nanofluids of different concentrations and temperatures. *SN Appl. Sci.* 5, 337. doi:10.1007/s42452-023-05574-7

Borode, A., Tshephe, T., Olubambi, P., Sharifpur, M., and Meyer, J. (2024). Effects of temperature and nanoparticle mixing ratio on the thermophysical properties of GNP–Fe2O3 hybrid nanofluids: an experimental study with RSM and ANN modeling. *J. Therm. Analysis Calorim.* 2024, 1–25. doi:10.1007/S10973-024-13029-3

Borode, A. O., Ahmed, N. A., Olubambi, P. A., Sharifpur, M., and Meyer, J. P. (2021). Investigation of the thermal conductivity, viscosity, and thermal performance of graphene nanoplatelet-alumina hybrid nanofluid in a differentially heated cavity. *Front. Energy Res.* 9. doi:10.3389/fenrg.2021.737915

Campos, C., Vasco, D., Angulo, C., Burdiles, P. A., Cardemil, J., and Palza, H. (2019). About the relevance of particle shape and graphene oxide on the behavior of direct absorption solar collectors using metal based nanofluids under different radiation intensities. *Energy Convers. Manag.* 181, 247–257. doi:10.1016/J.ENCONMAN.2018.12.007

Dalkılıç, A. S., Yalçın, G., Küçükyıldırım, B. O., Öztuna, S., Akdoğan Eker, A., Jumpholkul, C., et al. (2018). Experimental study on the thermal conductivity of water-based CNT-SiO2 hybrid nanofluids. *Int. Commun. Heat Mass Transf.* 99, 18–25. doi:10.1016/J.ICHEATMASSTRANSFER.2018.10.002

Elshamy, S. M., El-Said, E. M. S., Panchal, H., and El-Tahan, H. R. (2021). Performance assessment of a solar water distiller using circular parabolic absorber: an experimental investigation. *Case Stud. Therm. Eng.* 28, 101508. doi:10.1016/J.CSITE.2021.101508

Elshazly, E., Abdel-Rehim, A. A., and El-Mahallawi, I. (2022). 4E study of experimental thermal performance enhancement of flat plate solar collectors using MWCNT, Al2O3, and hybrid MWCNT/Al2O3 nanofluids. *Results Eng.* 16, 100723. doi:10.1016/J.RINENG.2022.100723

Ganvir, R. B., Walke, P. V., and Kriplani, V. M. (2017). Heat transfer characteristics in nanofluid—a review. *Renew. Sustain. Energy Rev.* 75, 451–460. doi:10.1016/j.rser.2016.11.010

Gao, Y., Xi, Y., Yang, Z., Sasmito, A. P., Mujumdar, A. S., and Wang, L. (2021). Experimental investigation of specific heat of aqueous graphene oxide Al2O3 hybrid nanofluid. *Therm. Sci.* 25, 515–525. doi:10.2298/TSCI190404381G

Habchi, A., Hartiti, B., Labrim, H., Fadili, S., Faddouli, A., El hajjam, N., et al. (2023). Performance study of a new parabolic trough design under optical concentrator effect. *Appl. Therm. Eng.* 219, 119500. doi:10.1016/J.APPLTHERMALENG.2022.119500

Hawwash, A. A., Abdel Rahman, A. K., Nada, S. A., and Ookawara, S. (2018). Numerical investigation and experimental verification of performance enhancement of flat plate solar collector using nanofluids. *Appl. Therm. Eng.* 130, 363–374. doi:10.1016/j.applthermaleng.2017.11.027

Henein, S. M., and Abdel-Rehim, A. A. (2022). The performance response of a heat pipe evacuated tube solar collector using MgO/MWCNT hybrid nanofluid as a working fluid. *Case Stud. Therm. Eng.* 33, 101957. doi:10.1016/J.CSITE.2022.101957

Hosseini Esfahani, A., Aliehyaei, M., Joshaghani, A. H., and Najafizadeh, M. M. (2023). Energy, exergy, economic and environmental analysis of parabolic trough collector containing hybrid nanofluid equipped with turbulator. *Eng. Anal. Bound Elem.* 150, 492–506. doi:10.1016/J.ENGANABOUND.2023.02.031

Huminic, G., Huminic, A., Vărdaru, A., Dumitrache, F., and Fleacă, C. (2024). Experimental investigation on Ag NPs-rGO-water/ethylene-glycol hybrid nanofluids used in solar applications. *Diam. Relat. Mater* 143, 110851. doi:10.1016/J.DIAMOND.2024.110851

Huq, T., Ong, H. C., Chew, B. T., Kazi, S. N., Zubir, M. N. M., Ong, Z. C., et al. (2023). Graphene nanoplatelet nanofluids stabilised by hybridisation with graphene oxide: preparation, stability, and performance in flat plate solar thermal collector. *J. Therm. Anal. Calorim.* 148, 2105–2118. doi:10.1007/s10973-022-11866-8

Hussein, A. K., Rashid, F. L., Togun, H., Sultan, H. S., Homod, R. Z., Sadeq, A. M., et al. (2024). A review of design parameters, advancement, challenges, and mathematical modeling of asphalt solar collectors. *J. Therm. Anal. Calorim.* 149, 41–61. doi:10.1007/s10973-023-12674-4

Hussein, O. A., Habib, K., Muhsan, A. S., Saidur, R., Alawi, O. A., and Ibrahim, T. K. (2020). Thermal performance enhancement of a flat plate solar collector using hybrid nanofluid. *Sol. Energy* 204, 208–222. doi:10.1016/J.SOLENER.2020.04.034

Ibrahim, I. U., Sharifpur, M., Meyer, J. P., and Murshed, S. M. S. (2024). Experimental investigations of effects of nanoparticle size on force convective heat transfer characteristics of Al2O3 - MWCNT hybrid nanofluids in transitional flow regime. *Int. J. Heat. Mass Transf.* 228, 125597. doi:10.1016/J.IJHEATMASSTRANSFER.2024.125597

Ibrahim, M., Abidi, A., Algehyne, E. A., Saeed, T., Cheraghian, G., and Sharifpur, M. (2022). Improvement of the energy and exergy efficiencies of the parabolic solar collector equipped with a twisted turbulator using SWCNT-Cu/water two-phase hybrid nanofluid. *Sustain. Energy Technol. Assessments* 49, 101705. doi:10.1016/J.SETA.2021.101705

Ibrahim, M., Berrouk, A. S., Algehyne, E. A., Saeed, T., and Chu, Y. M. (2021). Numerical evaluation of exergy efficiency of innovative turbulators in solar collector filled with hybrid nanofluid. *J. Therm. Anal. Calorim.* 145, 1559–1574. doi:10.1007/s10973-021-10759-6

Ilyas, S. U., Shamsuddin, R., Kai Xiang, T., Estellé, P., and Pendyala, R. (2023). Rheological profile of graphene-based nanofluids in thermal oil with hybrid additives of carbon nanotubes and nanofibers. *J. Mol. Liq.* 376, 121443. doi:10.1016/J.MOLLIQ.2023.121443

Jin, W., Jiang, L., Lv, Y., Li, K., Liu, H., Cao, W., et al. (2024). Experimental study on preparation and heat transfer efficiency of ethylene glycol/water-based hybrid nanofluids enhanced by graphene oxide/MXene nanoparticles. *J. Mol. Liq.* 405, 125033. doi:10.1016/J.MOLLIQ.2024.125033

Kanti, P., Sharma, K. V., Khedkar, R. S., and Rehman, T. R. (2022). Synthesis, characterization, stability, and thermal properties of graphene oxide based hybrid nanofluids for thermal applications: experimental approach. *Diam. Relat. Mater.* 128, 109265. doi:10.1016/J.DIAMOND.2022.109265

Kanti, P. K., and Maiya, M. P. (2022). Rheology and thermal conductivity of graphene oxide and coal fly ash hybrid nanofluids for various particle mixture ratios for heat transfer applications: experimental study. *Int. Commun. Heat Mass Transf.* 138, 106408. doi:10.1016/J.ICHEATMASSTRANSFER.2022.106408

Kanti, P. K., Sharma, P., Koneru, B., Banerjee, P., and Jayan, K. D. (2023a). Thermophysical profile of graphene oxide and MXene hybrid nanofluids for sustainable energy applications: model prediction with a Bayesian optimized neural network with K-cross fold validation. *FlatChem* 39, 100501. doi:10.1016/J.FLATC.2023.100501

Kanti, P. K., Sharma, P., Maiya, M. P., and Sharma, K. V. (2023b). The stability and thermophysical properties of Al2O3-graphene oxide hybrid nanofluids for solar energy

applications: application of robust autoregressive modern machine learning technique. *Sol. Energy Mater. Sol. Cells* 253, 112207. doi:10.1016/j.solmat.2023.112207

Kanti, P. K., Vicki Wanatasanappan, V., Mahjoub Said, N., and Sharma, K. V. (2024). Stability, thermophysical properties, forced convective heat transfer, entropy minimization and exergy performance of a novel hybrid nanofluid: experimental study. *J. Mol. Liq.* 410, 125571. doi:10.1016/J.MOLLIQ.2024.125571

Karami, M., Raisee, M., and Delfani, S. (2014). Numerical investigation of nanofluid-based solar collectors. *IOP Conf. Ser. Mater Sci. Eng.* 64, 012044. doi:10.1088/1757-899X/64/1/012044

Kassem, A., Al-Haddad, K., Komljenovic, D., and Schiffauerova, A. (2016). A value tree for identification of evaluation criteria for solar thermal power technologies in developing countries. *Sustain. Energy Technol. Assessments* 16, 18–32. doi:10.1016/J.SETA.2016.02.003

Kazemi, I., Sefid, M., and Afrand, M. (2020). Improving the thermal conductivity of water by adding mono and hybrid nano-additives containing graphene and silica: a comparative experimental study. *Int. Commun. Heat Mass Transf.* 116, 104648. doi:10.1016/J.ICHEATMASSTRANSFER.2020.104648

Khaledi, O., Saedodin, S., and Rostamian, S. H. (2022). Energy, hydraulic and exergy analysis of a compound parabolic concentrator using hybrid nanofluid: an experimental study. *Int. Commun. Heat Mass Transf.* 136, 106181. doi:10.1016/J.ICHEATMASSTRANSFER.2022.106181

Khan, M. S., Abid, M., Yan, M., Ratlamwala, T. A. H., and Mubeen, I. (2021). Thermal and thermodynamic comparison of smooth and convergent-divergent parabolic trough absorber tubes with the application of mono and hybrid nanofluids. *Int. J. Energy Res.* 45, 4543–4564. doi:10.1002/ER.6123

Khetib, Y., Alzaed, A., Tahmasebi, A., Sharifpur, M., and Cheraghian, G. (2022). Influence of using innovative turbulators on the exergy and energy efficacy of flat plate solar collector with DWCNTs-TiO2/water nanofluid. *Sustain. Energy Technol. Assessments* 51, 101855. doi:10.1016/J.SETA.2021.101855

Kishore, P. S., Sireesha, V., Harsha, V. S., Rao, V. D., and Solomon, A. B. (2020). Preparation, characterization and thermo-physical properties of Cu-graphene nanoplatelets hybrid nanofluids. *Mater Today Proc.* 27, 610–614. doi:10.1016/J.MATPR.2019.12.108

Kumar, V., Pare, A., Tiwari, A. K., and Ghosh, S. K. (2021). Efficacy evaluation of oxide-MWCNT water hybrid nanofluids: an experimental and artificial neural network approach. *Colloids Surf. A Physicochem Eng. Asp.* 620, 126562. doi:10.1016/j.colsurfa.2021.126562

Kumar, V., and Sarkar, J. (2020). Particle ratio optimization of Al2O3-MWCNT hybrid nanofluid in minichannel heat sink for best hydrothermal performance. *Appl. Therm. Eng.* 165, 114546. doi:10.1016/j.applthermaleng.2019.114546

Kumar Kanti, P., Sharma, P., Sharma, K. V., and Maiya, M. P. (2023). The effect of pH on stability and thermal performance of graphene oxide and copper oxide hybrid nanofluids for heat transfer applications: application of novel machine learning technique. *J. Energy Chem.* 82, 359–374. doi:10.1016/J.JECHEM.2023.04.001

Kumar, K. P., Deepthi Jayan, K., Sharma, P., and Alruqi, M. (2024). Thermo-electro-rheological properties of graphene oxide and MXene hybrid nanofluid for vanadium redox flow battery: application of explainable ensemble machine learning with hyperparameter optimization. *FlatChem* 43, 100606. doi:10.1016/J.FLATC.2023.100606

Lee, M., Shin, Y., and Cho, H. (2020). Performance evaluation of flat plate and vacuum tube solar collectors by applying a MWCNT/Fe₃O₄ binary nanofluid. *Energies* 13, 13–1715. doi:10.3390/EN13071715

Lee, M., Shin, Y., and Cho, H. (2021). Theoretical study on performance comparison of various solar collectors using binary nanofluids. *J. Mech. Sci. Technol.* 35 (3 35), 1267–1278. doi:10.1007/S12206-021-0238-4

Li, W., Zeng, Z., Le, S. J., Zhu, K., Huang, X., Hegab, H., et al. (2024). Investigation of a green nanofluid added with graphene and Al2O3 nano-additives for grinding hard-to-cut materials. *Tribol. Int.* 195, 109580. doi:10.1016/J.TRIBOINT.2024.109580

Li, X., Zeng, G., and Lei, X. (2020). The stability, optical properties and solar-thermal conversion performance of SiC-MWCNTs hybrid nanofluids for the direct absorption solar collector (DASC) application. *Sol. Energy Mater. Sol. Cells* 206, 110323. doi:10.1016/J.SOLMAT.2019.110323

Mashhadian, A., Heyhat, M. M., and Mahian, O. (2021). Improving environmental performance of a direct absorption parabolic trough collector by using hybrid nanofluids. *Energy Convers. Manag.* 244, 114450. doi:10.1016/J.ENCONMAN.2021.114450

Mehrali, M., Ghatkesar, M. K., and Pecnik, R. (2018). Full-spectrum volumetric solar thermal conversion via graphene/silver hybrid plasmonic nanofluids. *Appl. Energy* 224, 103–115. doi:10.1016/J.APENERGY.2018.04.065

Mehrali, M., Sadeghinezhad, E., Akhiani, A. R., Tahan Latibari, S., Metselaar, H. S. C., Kherbeet, A. S., et al. (2017). Heat transfer and entropy generation analysis of hybrid graphene/Fe3O4 ferro-nanofluid flow under the influence of a magnetic field. *Powder Technol.* 308, 149–157. doi:10.1016/J.POWTEC.2016.12.024

Moghadam, I. P., Afrand, M., Hamad, S. M., Barzinjy, A. A., and Talebizadehsardari, P. (2020). Curve-fitting on experimental data for predicting the thermal-conductivity of a new generated hybrid nanofluid of graphene oxide-titanium oxide/water. *Phys. A Stat. Mech. its Appl.* 548, 122140. doi:10.1016/j.physa.2019.122140

Mohammed, H. A., Vuthaluru, H. B., and Liu, S. (2021). Heat transfer augmentation of parabolic trough solar collector receiver's tube using hybrid nanofluids and conical turbulators. *J. Taiwan Inst. Chem. Eng.* 125, 215–242. doi:10.1016/J.JTICE.2021.06.032

Nabi, H., Pourfallah, M., Gholinia, M., and Jahanian, O. (2022). Increasing heat transfer in flat plate solar collectors using various forms of turbulence-inducing elements and CNTs-CuO hybrid nanofluids. *Case Stud. Therm. Eng.* 33, 101909. doi:10.1016/J.CSITE.2022.101909

Negeed, E. S. R., Alhazmy, M., Bokhary, A. Y. F., Abulkhair, H., Almas, M. A., and Hedia, H. S. (2023). Numerical simulation of flat plate solar collector equipped with a turbulator containing water/copper-graphene hybrid nanofluid utilizing a two-phase model. *Eng. Anal. Bound Elem.* 156, 90–113. doi:10.1016/J.ENGANABOUND.2023.08.006

Obalalu, A. M., Memon, M. A., Olayemi, O. A., Olilima, J., and Fenta, A. (2023). Enhancing heat transfer in solar-powered ships: a study on hybrid nanofluids with carbon nanotubes and their application in parabolic trough solar collectors with electromagnetic controls. *Sci. Rep.* 13 (1 13), 9476–9520. doi:10.1038/s41598-023-36716-x

Panchal, H., Sadasivuni, K. K., Suresh, M., Israr, M., and Sengottain, S. (2022). A concise review on Solar still with parabolic trough collector. *Int. J. Ambient Energy* 43, 4812–4819. doi:10.1080/01430750.2021.1922938

Patel, D. K., Brahmbhatt, P. K., and Panchal, H. (2018). A review on compound parabolic solar concentrator for sustainable development. *Int. J. Ambient Energy* 39, 533–546. doi:10.1080/01430750.2017.1318786

Qu, J., Zhang, R., Wang, Z., and Wang, Q. (2019). Photo-thermal conversion properties of hybrid CuO-MWCNT/H2O nanofluids for direct solar thermal energy harvest. *Appl. Therm. Eng.* 147, 390–398. doi:10.1016/J.APPLTHERMALENG.2018.10.094

Ranga Babu, J. A., Kumar, K. K., and Srinivasa Rao, S. (2017). State-of-art review on hybrid nanofluids. *Renew. Sustain. Energy Rev.* 77, 551–565. doi:10.1016/j.rser.2017.04.040

Ranjbarzadeh, R., Akhgar, A., Musivand, S., and Afrand, M. (2018). Effects of graphene oxide silicon oxide hybrid nanomaterials on rheological behavior of water at various time durations and temperatures: synthesis, preparation and stability. *Powder Technol.* 335, 375–387. doi:10.1016/J.POWTEC.2018.05.036

Razavi Dehkordi, M. H., Alizadeh, A., Zekri, H., Rasti, E., Kholoud, M. J., Abdollahi, A., et al. (2023). Experimental study of thermal conductivity coefficient of GNSs-WO3/LP107160 hybrid nanofluid and development of a practical ANN modeling for estimating thermal conductivity. *Heliyon* 9, e17539. doi:10.1016/J.HELIYON.2023.E17539

Rostami, S., Nadooshan, A. A., and Raisi, A. (2019). An experimental study on the thermal conductivity of new antifreeze containing copper oxide and graphene oxide nano-additives. *Powder Technol.* 345, 658–667. doi:10.1016/J.POWTEC.2019.01.055

Rovira, A., Barbero, R., Montes, M. J., Abbas, R., and Varela, F. (2016). Analysis and comparison of Integrated Solar Combined Cycles using parabolic troughs and linear Fresnel reflectors as concentrating systems. *Appl. Energy* 162, 990–1000. doi:10.1016/J.APENERGY.2015.11.001

Saddouri, I., Rejeb, O., Semmar, D., and Jemni, A. (2023). A comparative analysis of parabolic trough collector (PTC) using a hybrid nanofluid. *J. Therm. Anal. Calorim.* 148, 9701–9721. doi:10.1007/s10973-023-12342-7

Said, Z., Abdelkareem, M. A., Rezk, H., Nassef, A. M., and Atwany, H. Z. (2020). Stability, thermophysical and electrical properties of synthesized carbon nanofiber and reduced-graphene oxide-based nanofluids and their hybrid along with fuzzy modeling approach. *Powder Technol.* 364, 795–809. doi:10.1016/J.POWTEC.2020.02.026

Said, Z., Sharma, P., Syam Sundar, L., Afzal, A., and Li, C. (2021). Synthesis, stability, thermophysical properties and AI approach for predictive modelling of Fe3O4 coated MWCNT hybrid nanofluids. *J. Mol. Liq.* 340, 117291. doi:10.1016/j.molliq.2021.117291

Saleh, B., and Sundar, L. S. (2021). Thermal efficiency, heat transfer, and friction factor analyses of MWCNT + Fe3O4/water hybrid nanofluids in a solar flat plate collector under thermosyphon condition. *Processes* 9, 180. Page 180 9, 180. doi:10.3390/PR9010180

Sarbolookzadeh Harandi, S., Karimipour, A., Afrand, M., Akbari, M., and D'Orazio, A. (2016). An experimental study on thermal conductivity of F-MWCNTs–Fe 3 O 4/EG hybrid nanofluid: effects of temperature and concentration. *Int. Commun. Heat Mass Transf.* 76, 171–177. doi:10.1016/j.icheatmasstransfer.2016.05.029

Selvarajoo, K., Wanatasanappan, V. V., and Luon, N. Y. (2024). Experimental measurement of thermal conductivity and viscosity of Al2O3-GO (80:20) hybrid and mono nanofluids: a new correlation. *Diam. Relat. Mater* 144, 111018. doi:10.1016/J.DIAMOND.2024.111018

Shahsavar, A., Salimpour, M. R., Saghafian, M., and Shafii, M. B. (2015). An experimental study on the effect of ultrasonication on thermal conductivity of ferrofluid loaded with carbon nanotubes. *Thermochim. Acta* 617, 102–110. doi:10.1016/J.TCA.2015.08.025

Shajan, S., Baiju, V., Krishnakumar, T. S., Andrew, G., Thomas, L., Alex, M., et al. (2021). Experimental investigation on thermophysical properties of Therminol® 55 based hybrid nanofluids with alumina and graphene nanoplatelets for medium temperature applications. *Therm. Sci. Eng. Prog.* 26, 101116. doi:10.1016/J.TSEP.2021.101116

Shende, R., and Sundara, R. (2015). Nitrogen doped hybrid carbon based composite dispersed nanofluids as working fluid for low-temperature direct absorption solar collectors. *Sol. Energy Mater. Sol. Cells* 140, 9–16. doi:10.1016/J.SOLMAT.2015.03.012

Shin, Y., Ham, J., Boldoo, T., and Cho, H. (2020). Magnetic effect on the enhancement of photo-thermal energy conversion efficiency of MWCNT/Fe3O4 hybrid nanofluid. *Sol. Energy Mater. Sol. Cells* 215, 110635. doi:10.1016/J.SOLMAT.2020.110635

Siddiqui, F. R., Tso, C. Y., Fu, S. C., Qiu, H. H., and Chao, C. Y. H. (2021). Droplet evaporation and boiling for different mixing ratios of the silver-graphene hybrid nanofluid over heated surfaces. *Int. J. Heat. Mass Transf.* 180, 121786. doi:10.1016/J.IJHEATMASSTRANSFER.2021.121786

Singh, P. K., Manikandan, R., Kumar, R., Verma, R., Kulandaivel, A., Kamesh, V. V., et al. (2024). Enhancing thermal energy and exergy harvesting in concentrated solar power systems using graphene-ZrO2/water hybrid nanofluid: an experimental study. *Process Saf. Environ. Prot.* 191, 1461–1471. doi:10.1016/J.PSEP.2024.09.028

Soltani, F., Toghraie, D., and Karimipour, A. (2020). Experimental measurements of thermal conductivity of engine oil-based hybrid and mono nanofluids with tungsten oxide (WO3) and MWCNTs inclusions. *Powder Technol.* 371, 37–44. doi:10.1016/J.POWTEC.2020.05.059

Sreekumar, S., Ganguly, A., Khalil, S., Chakrabarti, S., Hewitt, N., Mondol, J. D., et al. (2024). Thermo-optical characterization of novel MXene/Carbon-dot hybrid nanofluid for heat transfer applications. *J. Clean. Prod.* 434, 140395. doi:10.1016/J.JCLEPRO.2023.140395

Srinivasan, N. kumar, and Ponnusamy, C. (2024). Stability, thermal and solidification behaviour of oxygen functionalized GNPs–CuO/water-based hybrid nanofluid phase change materials for cool thermal energy storage system. *J. Energy Storage* 98, 113107. doi:10.1016/J.EST.2024.113107

Struchalin, P. G., Kuzmenkov, D. M., Yunin, V. S., Wang, X., He, Y., and Balakin, B. V. (2022). Hybrid nanofluid in a direct absorption solar collector: magnetite vs. Carbon nanotubes compete for thermal performance. *Energies* 15, 1604. doi:10.3390/EN15051604

Syam Sundar, L., Singh, M. K., Ferro, M. C., and Sousa, A. C. M. (2017). Experimental investigation of the thermal transport properties of graphene oxide/Co$_3$O$_4$ hybrid nanofluids. *Int. Commun. Heat Mass Transf.* 84, 1–10. doi:10.1016/J.ICHEATMASSTRANSFER.2017.03.001

Taherialekouhi, R., Rasouli, S., and Khosravi, A. (2019). An experimental study on stability and thermal conductivity of water-graphene oxide/aluminum oxide nanoparticles as a cooling hybrid nanofluid. *Int. J. Heat. Mass Transf.* 145, 118751. doi:10.1016/J.IJHEATMASSTRANSFER.2019.118751

Tahmasebi, A., Abed, A. M., Aghaei, A., Izadi, F., Malekshah, E. H., and Aybar, H. (2023). Investigation into the effect of twisted tape on the thermo-hydraulic performance and entropy generation of turbulent flow of mono and hybrid magnetic nanofluids inside a parabolic solar collector absorber tube by applying two-phase analysis. *Eng. Anal. Bound Elem.* 150, 318–328. doi:10.1016/J.ENGANABOUND.2023.02.007

Tiwari, A. K., Pandya, N. S., Shah, H., and Said, Z. (2023). Experimental comparison of specific heat capacity of three different metal oxides with MWCNT/water-based hybrid nanofluids: proposing a new correlation. *Appl. Nanosci. Switz.* 13, 189–199. doi:10.1007/s13204-020-01578-6

Tong, Y., Boldoo, T., Ham, J., and Cho, H. (2020). Improvement of photo-thermal energy conversion performance of MWCNT/Fe3O4 hybrid nanofluid compared to Fe3O4 nanofluid. *Energy* 196, 117086. doi:10.1016/J.ENERGY.2020.117086

Van Trinh, P., Anh, N. N., Hong, N. T., Hong, P. N., Minh, P. N., and Thang, B. H. (2018). Experimental study on the thermal conductivity of ethylene glycol-based nanofluid containing Gr-CNT hybrid material. *J. Mol. Liq.* 269, 344–353. doi:10.1016/J.MOLLIQ.2018.08.071

Vărdaru, A., Huminic, G., Huminic, A., Fleacă, C., Dumitrache, F., and Morjan, I. (2022). Synthesis, characterization and thermal conductivity of water based graphene oxide–silicon hybrid nanofluids: an experimental approach. *Alexandria Eng. J.* 61, 12111–12122. doi:10.1016/J.AEJ.2022.06.012

Vărdaru, A., Huminic, G., Huminic, A., Fleacă, C., Dumitrache, F., and Morjan, I. (2023). Aqueous hybrid nanofluids containing silver-reduced graphene oxide for improving thermo-physical properties. *Diam. Relat. Mater* 132, 109688. doi:10.1016/J.DIAMOND.2023.109688

Verma, S. K., Tiwari, A. K., Tiwari, S., and Chauhan, D. S. (2018). Performance analysis of hybrid nanofluids in flat plate solar collector as an advanced working fluid. *Sol. Energy* 167, 231–241. doi:10.1016/J.SOLENER.2018.04.017

Wang, J., Li, G., Li, T., Zeng, M., and Sundén, B. (2021). Effect of various surfactants on stability and thermophysical properties of nanofluids. *J. Therm. Anal. Calorim.* 143, 4057–4070. doi:10.1007/s10973-020-09381-9

Wang, Y., Xu, J., Liu, Q., Chen, Y., and Liu, H. (2016). Performance analysis of a parabolic trough solar collector using Al2O3/synthetic oil nanofluid. *Appl. Therm. Eng.* 107, 469–478. doi:10.1016/J.APPLTHERMALENG.2016.06.170

Yarmand, H., Gharehkhani, S., Ahmadi, G., Shirazi, S. F. S., Baradaran, S., Montazer, E., et al. (2015). Graphene nanoplatelets–silver hybrid nanofluids for enhanced heat transfer. *Energy Convers. Manag.* 100, 419–428. doi:10.1016/J.ENCONMAN.2015.05.023

Yarmand, H., Gharehkhani, S., Shirazi, S. F. S., Amiri, A., Montazer, E., Arzani, H. K., et al. (2016a). Nanofluid based on activated hybrid of biomass carbon/graphene oxide: synthesis, thermo-physical and electrical properties. *Int. Commun. Heat Mass Transf.* 72, 10–15. doi:10.1016/J.ICHEATMASSTRANSFER.2016.01.004

Yarmand, H., Gharehkhani, S., Shirazi, S. F. S., Goodarzi, M., Amiri, A., Sarsam, W. S., et al. (2017b). Study of synthesis, stability and thermo-physical properties of graphene nanoplatelet/platinum hybrid nanofluid. *Int. Commun. Heat Mass Transf.* 77, 15–21. doi:10.1016/j.icheatmasstransfer.2016.07.010

Zadkhast, M., Toghraie, D., and Karimipour, A. (2017). Developing a new correlation to estimate the thermal conductivity of MWCNT-CuO/water hybrid nanofluid via an experimental investigation. *J. Therm. Anal. Calorim.* 129, 859–867. doi:10.1007/s10973-017-6213-8

Zeng, J., and Xuan, Y. (2018). Enhanced solar thermal conversion and thermal conduction of MWCNT-SiO2/Ag binary nanofluids. *Appl. Energy* 212, 809–819. doi:10.1016/J.APENERGY.2017.12.083

Zheng, N., Yan, F., Wang, L., and Sun, Z. (2022). Photo-thermal conversion performance of mono MWCNT and hybrid MWCNT-TiN nanofluids in direct absorption solar collectors. *Int. J. Energy Res.* 46, 8313–8327. doi:10.1002/ER.7730

Nomenclature

CNTs	Carbon nanotubes
CF-CNTs	Chemically functionalized carbon nanotubes
CF-GNPs	Functionalised graphene nanoplatelets
CMCNa	Sodium carboxymethyl cellulose
Cp	Specific heat capacity
CT	Cetyltrimethylammonium bromide
DASC	Direct absorption solar collector
EG	Ethylene glycol
FPSC	Flat plate solar collector
GO	Graphene oxide
GNP	Graphene nanoplatelet
hBN	Hexagonal boron nitride
HNF	Hybrid nanofluid
HTF	Heat transfer fluid
MWCNT	Multi-walled carbon nanotube
NFPCM	Nanofluid phase change material
PEG	Polyethylene glycol
PTC	Parabolic trough collector
PTSC	Parabolic trough solar collector
rGO	Reduced graphene oxide
SHC	Specific heat capacity
SLS	Sodium lauryl sulfate
TC	Thermal conductivity
TCR	Thermal conductivity ratio
TIG	Innovative turbulator geometries
TT	Twisted tape
VUSC	Vacuum tube solar collector
W	Water